LIMNOLOGY and OCEANOGRAPHY

ASLO

*Limnol. Oceanogr.* 9999, 2021, 1–18
© 2020 Association for the Sciences of Limnology and Oceanography
doi: 10.1002/lno.11663

# Biogeochemical characteristics and hydroperiod affect carbon dioxide flux rates from exposed high-elevation pond sediments

**Amanda Gay DelVecchia** [1,2*,a] **Steven Gougherty,** [1,2,b] **Brad W. Taylor** [1,2] **Scott A. Wissinger** [2,3,†]

[1]Department of Applied Ecology, North Carolina State University, Raleigh, North Carolina
[2]Rocky Mountain Biological Laboratory, Crested Butte, Colorado
[3]Biology and Environmental Science Departments, Allegheny College, Meadville, Pennsylvania

## *Abstract*

While inundated, small ponds (< 1000 $m^2$ area) account for disproportionately large contributions of $CO_2$ efflux to the global carbon budget and also store carbon in anoxic sediments. However, pond hydrology is shifting toward increasingly dry conditions in alpine and temperate zones, which might lead to increased exposure of shallow pond sediments. We analyzed sediment $CO_2$ efflux rates in dried sediments of multiple ponds of varying hydrology and sediment characteristics at montane and subalpine elevations near the Rocky Mountain Biological Laboratory in Colorado. Average $CO_2$ efflux rates from exposed sediments, 331.5 ± 11.5 mmol $m^{-2}$ $d^{-1}$ at the montane sites and 142.8 ± 45.1 mmol $m^{-2}$ $d^{-1}$ at the subalpine sites, were 10 times higher than average $CO_2$ efflux rates from pond water. Principal components analysis to reduce dimensionality of sediment characteristics revealed that random inter-pond differences rather than exposure timing or hydroperiod drove variation among sediments. In linear mixed effects models of $CO_2$ flux rates, significant predictors included sediment moisture and temperature, pH, total organic carbon, and organic matter content at all pond hydroperiod classifications and sites. However, the sediment characteristics explaining the most variance differed among sites and hydroperiods and included nitrate concentrations, pH, bulk density, and temperature. We conclude that pond sediments are heterogeneous both within and among ponds in close proximity, and drivers of relatively high $CO_2$ efflux rates differ among pond hydroperiods and elevations. This work emphasizes that local differences can impact predictions of $CO_2$ flux from lentic sediments which are becoming increasingly exposed.

Though comprising a small portion of global surface area, inland waters are an important component of the global carbon budget because they have high rates of gaseous carbon efflux as well as high rates of carbon storage in sediments (Duarte and Prairie 2005; Cole et al. 2007). In particular, small ponds (< 1000 $m^2$) embedded in terrestrial landscapes comprise only 8.6% of global lentic surface area, but account for 15.1% of total $CO_2$ emissions from lentic systems (Holgerson and Raymond 2016). Small ponds, wetlands, and other shallow lentic habitats are also carbon cycling hotpots because they have high inputs of terrestrial and aquatic vascular plant carbon, high rates of organic carbon stored in sediments, and high surface area to volume ratios (Downing et al. 2006; Cole et al. 2007).

While inundated, shallow standing water habitats provide a net efflux of $CO_2$ and store substantial organic carbon in anoxic sediments, leading to organic carbon burial rates that are higher than most other terrestrial and aquatic system types (Taylor et al. 2019). When pond sediments are exposed to the atmosphere, they become aerated, which can stimulate aerobic microbial processes and rapid efflux of carbon dioxide (e.g. Fromin et al. 2010). Although most studies of small pond $CO_2$ efflux consider only the pond waters themselves, a few studies of dried temporary ponds have shown that exposed pond sediments can release more carbon dioxide than the waters had released while the sediment was inundated (Catalán et al. 2014; Obrador et al. 2018; DelVecchia et al. 2019). The tradeoff between carbon burial under anoxic conditions during the inundated phase of pond sediments vs. aerobic respiration and abiotic transport processes (Rey 2015) during sediment exposure to air suggests that pond hydrology could affect overall pond $CO_2$ flux rates both directly and by influencing sediment characteristics.

*Correspondence: amanda.delvecchia@duke.edu

Additional Supporting Information may be found in the online version of this article.

[a]Present address: Nicholas School of the Environment, Duke University, Durham, North Carolina, USA
[b]Present address: Department of Biology, Boston University, Boston, Massachusetts, USA

[†]Author deceased October 5, 2019.

[Corrections added on 28 December 2020, after first online publication: affliation and present address updated.]

Pond hydroperiods are defined by the frequency and duration of annual pond inundation vs. exposure. Temporary ponds are defined as those that have a recurring (annual) dry phase (Williams 1997), but the dry phase can vary spatially (whole pond vs. a subset of basin margins) and temporally across years. Semi-permanent ponds dry completely in some but not all years depending on annual snowpack and rainfall (Batzer et al. 1999; Wissinger et al. 1999). In boreal, temperate and alpine systems, the frequency and magnitude of pond drying is increasing because climate change has already, and is predicted to continue, shifting temperate and alpine wetland hydrology toward early melting, increasingly dry conditions by decreasing snowpack, water supply and increasing evaporative losses (Burkett and Kusler 2000; Clow 2010; Lee et al. 2015). Warmer winters in particular lead to a lower amount of snowpack (Barnett et al. 2005), and warmer annual temperatures and a shorter duration of snow cover allow for greater evaporation (Carpenter et al. 1992; Arnell 1999). As a result, snowmelt-driven ponds at high latitudes and elevations are drying earlier in the season and more frequently (Smol and Douglas 2007; Wissinger et al. 2016).

These conditions have the potential to release stored carbon by facilitating microbe, macro-organism, and root respiration in previously submerged sediments (Ryan and Law 2005). Small ponds have higher ratios of perimeter to surface area and littoral sediments are located in close proximity to terrestrial vegetation, thus they might contain a terrestrial root component to respiration, similar to soils. In soils, approximately half of respiration has been attributed to metabolic activity associated with growing roots and associated mycorrhizae, and the majority of the remaining half to heterotrophic microbial respiration based on recently produced organic material (Trumbore 2000; Ryan and Law 2005).

Soil and sediment respiration rates have known relationships to temperature and moisture. Temperature can affect root-related and microbe-related respiration rates differently (Boone et al. 1998) but $CO_2$ efflux generally increases exponentially with temperature (Fang and Moncrieff 2001). Carbon dioxide flux rates also decrease linearly with gravimetric moisture content and log-linearly with moisture potential, although both of these relationships can vary with substrate availability at the lowest or highest values of moisture content (Orchard and Cook 1983; Davidson et al. 1998; Fang and Moncrieff 2001). This relationship can also vary if sediment moisture reflects a rewetting event, because rewetting has been shown to increase rates of $CO_2$ efflux, perhaps by creating osmotic shock in microbial cells and releasing labile dissolved organic carbon for respiration by surviving microbes (Fierer and Schimel 2003), by displacing $CO_2$ from pore spaces (Gallo et al. 2014), or by enhancing decomposition (Birch 1959; Jarvis et al. 2007). Moisture and temperature are interacting factors affecting respiration because high water content can impede oxygen diffusion, inhibiting decomposition and associated $CO_2$ production regardless of temperature (Skopp et al. 1990; Davidson et al. 1998), but desiccation can impact microbial activity and cause dormancy or mortality (Shukla and Varma 2010).

Carbon dioxide flux rates can also be related to organic matter and nutrient content, which provide substrate for respiration. For example, in a recent study of pond sediment and water $CO_2$ efflux rates, Obrador et al. (2018) found that rates were higher in sediments and waters with higher concentrations of humic organic matter. In other soil and sediment types, $CO_2$ flux rates are positively related to microbial biomass carbon and nitrogen content, and dissolved organic carbon and nitrogen content (subtropical forest sediments, Iqbal et al. 2010). Rates can also respond positively to additions of organic matter (tropical forest sediments, Cleveland et al. 2007). However, flux rate responses to carbon and nutrient content or additions are inconsistent at the global scale and can be outweighed by the effects of subsurface moisture (Raich and Schlesinger 1992; Schlesinger and Andrews 2000).

Factors that affect sediment $CO_2$ efflux are especially important in considering the carbon dynamics in snowmelt-driven ponds in boreal, temperate and alpine settings because these ponds dry down over the course of a season (from ice-out to refreezing) and sediments with varying characteristics become exposed to shifts in temperature and moisture over that time (Fig. 1). Despite the clear importance of small ponds in the global carbon budget (Holgerson and Raymond 2016), (1) pond $CO_2$ flux rates are generally calculated from wetted periods alone, lacking the potentially higher estimates that include exposed sediments; (2) we have little understanding of how the combination of pond hydrology and sediment characteristics affect sediment $CO_2$ flux rate; and (3) we have few baseline data for pond sediment $CO_2$ flux to understand how overall pond flux rates might shift with climate change (Marcé et al. 2019). There are two major temporal scales of pond hydrology that could affect exposed sediment $CO_2$ flux rates: pond sediments that dry more frequently on an inter-annual basis (i.e., temporary and semi-permanent ponds) might have lower accumulated organic matter over time because of frequent sediment aeration, which might be preferentially released from drying sediments (Weise et al. 2016; Gómez-Gener et al. 2016). Second, sediments in any pond hydroperiod differ in the timing of exposure to air, and sediments that are exposed to air later in the season each year might retain or accumulate more organic matter. Thus, we asked, (1) how do sediment characteristics relate to pond hydroperiods, (2) how do sediment characteristics relate to the timing of exposure to air, and connecting the two questions, (3) how do $CO_2$ flux rates from exposed sediments relate to sediment characteristics? In order to investigate these questions, we measured pond sediment $CO_2$ flux rates and characteristics across 19 ponds at two sites in Colorado (7 montane ponds and 12 subalpine ponds, Fig. 2). We chose the two sites because they differed in terms of elevation and nutrient input from cattle disturbance (none vs. annual grazing), and thus encompassed a range of sediment characteristics.

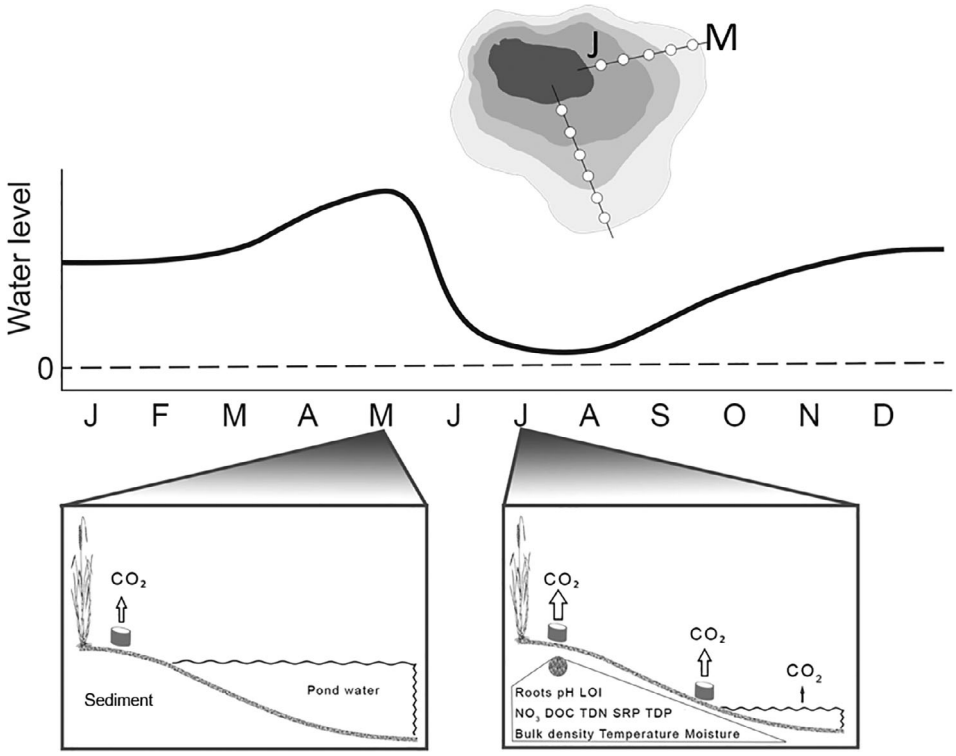



**Fig 1.** A conceptual hydrograph for these snowmelt driven ponds shows melt-out in spring. Ponds then steadily dry down over the course of the season until they refill with snow in late fall. As ponds dry down, they expose margins of sediment from which we collected estimates of $CO_2$ flux. Upper figure conceptual overview of a pond shows how pond margins might shrink over time from May (M) to July (J) and how transects were oriented toward the deepest part of the pond (gauged by the shrinking pond margins) with collars placed progressively as the pond water area shrunk. We considered direct effects of hydrology (exposure date and associated temperature and moisture) as well as how overall hydrologic patterns could affect sediment characteristics which might then influence $CO_2$ flux.

## *Study sites*

The subalpine (3640 m) cluster of ponds we studied is located in the Mexican Cut Nature Preserve (MCNP) in the Elk Mountains of Colorado. The site was well-suited to address our goals because it contains over 50 ponds of varying hydroperiods (degree of permanence and timing of melting and drying) that occur in close proximity to each other on bedrock at the upper edge of a coniferous tree line and are mainly replenished by snowmelt in spring. Long-term monitoring indicates that (1) permanent ponds have not dried during the past 50 years; (2) semi-permanent ponds dry in late summer in most, but not all years; and (3) temporary ponds dry annually in early to mid-summer (Wissinger et al. 1999, 2003). Temporary ponds tend to be shallower and have flatter basin shapes.

The ponds in the montane (2850 m elevation) cluster are kettles embedded in a mid-valley moraine in the East River Valley near the RMBL and surrounding vegetation is sparse (Wissinger et al. 2018). These shallow (< 1 m) isolated basins are always (since 1988) dry at the beginning of snow-pack accumulation in late autumn, and then fill with snowmelt in spring. Temporary basins dry annually in mid-summer (June–July) and semi-permanent basins dry in most (28 of the past 30) years by September with considerable inter-annual variability depending on snowpack, dates of snow melt, and summer rain (Wissinger et al. 2018). The ice-off and drying dates of these montane ponds is typically 4–6 weeks earlier than those at the subalpine pond cluster described above. During this study, the ponds thawed and had open water at the end of May in 2018 for the montane site and at the end of April in 2018 for the subalpine site.

High elevation life zones can generally have intermediate to high levels of soil carbon content relative to other systems globally, therefore playing an important role in the global carbon budget (Post et al. 1982). High elevation systems are also often considered to be sentinel systems for climate change at higher latitudes (Williamson et al. 2009; Wissinger et al. 2016). Still, high elevation ponds are often missing from assessments of small pond $CO_2$ concentrations and flux (Holgerson and Raymond 2016). Because they receive the majority of their annual precipitation as winter and spring snow, they are particularly vulnerable to shifts in the depth of snowpack and timing of melt (Serreze et al. 1999). The timing of snowmelt in this region has shifted a median of 2–3 weeks earlier between 1978 and 2007, with snow water equivalent declining by 3.6–4.1 cm $decade^{-1}$ (Clow et al. 2010). For

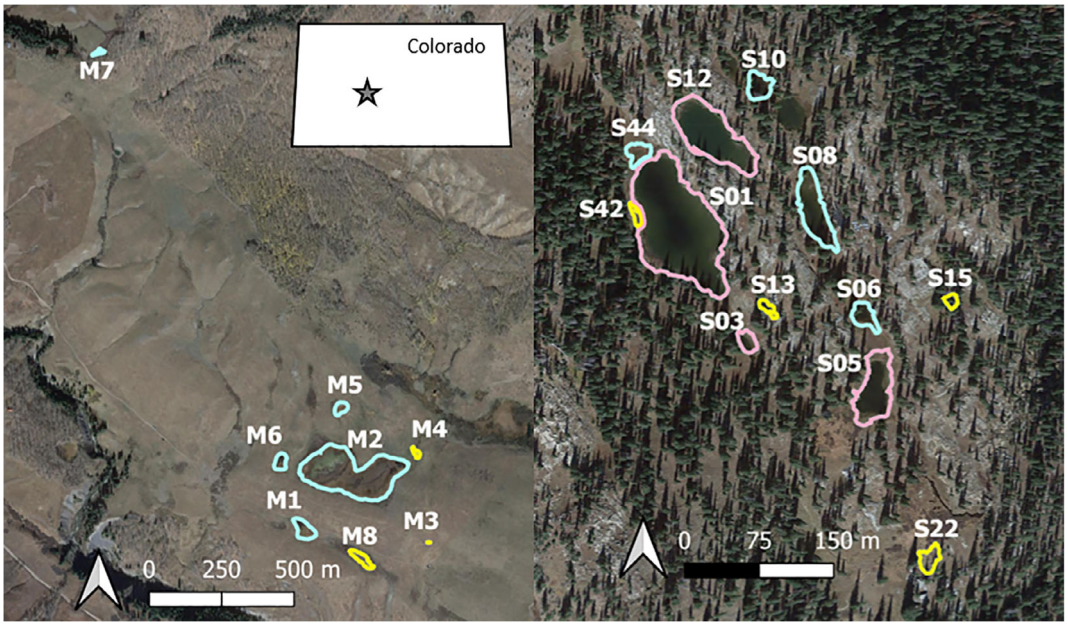



**Fig 2.** The southwest corner of the montane site (left) is located at 38°56′ 31″ N, 106°5846″ W and the southwest corner of the subalpine site (right) is located at 39°01′ 39″ N, 107°03′53″ W. Permanent ponds are in red, semi-permanent in blue, and temporary in yellow. [Color figure can be viewed at wileyonlinelibrary.com]

example, in 2012, snow depth was greater than 50 cm lower, snowmelt occurred 28 d earlier, and early summer precipitation was 12 cm less than the previous 10-year average across the region (Sexstone and Fassnacht 2014). In 2012 and other recent years with early snow melt, entire cohorts of species characterized as temporary-habitat specialists perished in the face of extraordinarily early pond drying at both study sites (Lund et al. 2016).

## Methods

### Measurement of sediment $CO_2$ flux rates

At each pond, we established two or three transects of sediment collars (10 cm diameter PVC cylinders), beginning at the southern end, moving to the western end, and occasionally adding others in the larger basins. We started by adding collars near the outermost wetted edge on each transect and gradually added additional collars toward the deeper water center on each transect as ponds dried down (Fig. 1). We were able to begin installing collars on June 5 at the montane site, and June 27 at the subalpine site in the outermost edges of ponds that had begun to dry down (Supporting Information Fig. 2). On these initial dates, we also installed three reference collars outside of ponds for comparison of $CO_2$ flux rates. These locations were chosen to be approximately the same elevation as the ponds but at least 20 m from pond margins.

We installed collars into exposed pond sediments by gently pushing and tapping in the collars evenly (total $n$ = 309). If vegetation was present (although it tended to be extremely minimal), we clipped it as low as possible to minimize autotrophic respiration in the samples and to allow for an airtight seal with the respiration chamber. We allowed the collars to sit for at least 24 h, and then measured collar height at four points on each collar. For a subset of these collars ($n$ = 136), we measured the collar heights again before removing them at the end of the measurement period. The change in collar heights over the course of the measurement period was negligible (coefficient of variation = 0.014).

We allowed at least 48 h to pass after collar installation before an initial measurement of $CO_2$ flux. We allowed this time to pass to prevent the disturbance caused by installing collar from affecting flux measurements. We measured rates of sediment $CO_2$ flux using a PP Systems EGM-5 Portable $CO_2$ Gas Analyzer equipped with an opaque respiration chamber (PP Systems, Amesbury, Massachusetts, hereafter referred to as SRC). At the time of each $CO_2$ flux measurement, we also measured sediment moisture (0–100% saturation) and sediment temperature using a HydraProbe II (Stevens Water Monitoring Systems) that was placed within 10 cm of each measured collar.

The SRC recirculated air within the chamber and through the instrument where $CO_2$ concentrations were measured. The SRC included a verification that the chamber was flushed before making measurements by recording ambient $CO_2$ concentrations within the chamber itself before beginning the measurement process. After a 110 s incubation period, a quadratic relationship was fit to the change in chamber $CO_2$ concentration over time by the instrument. This relationship provides a means of accounting for an

initial stabilization period and any leakage. The equation was as follows:

$$C = a + bt + ct^2$$

where $C$ is the concentration (ppm) in the chamber at time $t$ (s). Variables $a$, $b$, and $c$ are empirically determined coefficients for each chamber incubation. The true flux rate was calculated from $\partial C/\partial t$ at time $t = 0$. Thus, using $\partial C/\partial t = b + 2ct$, at $T = 0$, $\partial C/\partial t = b$. A comparison of $b$ and $ct$ yielded an estimate of leakage; $ct$ must be $< 20\%$ of $b$ or the relationship was deemed nonlinear by the instrument and we redid the chamber incubation.

At the montane pond site we measured sediment $CO_2$ efflux on the following dates and number of collars in 2018: 8 June ($n$ = 17), 11 June ($n$ = 17), 15 June ($n$ = 27), 25 June ($n$ = 28), 28 June ($n$ = 28), 9 July ($n$ = 50), and 16 July ($n$ = 46). At the subalpine site, we measured sediment $CO_2$ efflux on the following dates in 2018: 29 June ($n$ = 15), 5–6 July ($n$ = 34), 10 July ($n$ = 24), 13 July ($n$ = 34), 23–24 July ($n$ = 82), 30–31 July ($n$ = 85), 6–7 August ($n$ = 92), and 10–11 September ($n$ = 110).

**Measurement of drying dates and sediment characteristics**

We visited sites approximately twice weekly to flag new pond wetted area margins in order to assess the dates on which sediments became exposed, or the dates on which the water table first dropped below the sediment surface ("earliest exposure date"). Pond areas progressively retracted, gradually exposing more sediment, and thus collars with later exposure dates also tended to be located further into the interior of the pond (e.g., as demonstrated in Fig. 1), although we did not have distance to pond margin measurements during each time of sampling. Because the study sites were very exposed and dangerous during storms, in addition to being difficult to access easily and lacking precipitation gauges, we had no way of knowing explicitly what happened between visitation dates and thus collars might have been rewetted during this time. Although it was a dry summer in terms of snowpack, rain events occurred in July–September (https://www.usclimatedata.com/climate/crested-butte/colorado/united-states/usco0093). On July 11 and July 17, we removed collars from the montane ponds and in September we removed collars from the subalpine site ponds. We immediately collected sediment cores (5.6 cm diameter, 7 cm depth) from within the collars and transported them to the lab on ice, where they were refrigerated at 4°C for 12–24 h until ensuing analyses could be completed. We weighed samples to obtain a field moist mass for the entire sample, homogenized the moist sample by mixing, then allocated subsamples to different analyses.

We allocated 5 g of the sample to measuring gravimetric sediment moisture by drying the sample at 60°C for 48 h and measuring mass lost by drying. We calculated bulk density (BD) by multiplying the entire field moist sample mass by the dry-to-field moist ratio of the sediment (obtained from the gravimetric sediment moisture analysis) and dividing by the volume of the sediment core (172.41 $cm^3$). We measured sediment pH using the protocol of the Kellogg Biological Station that required two 15 g field-moist subsamples to be mixed in 30 mL of deionized water (DI) each for 30 min (Robertson et al. 1999). We used an Accumet AP62 pH meter (Fisher Scientific).

We used a DI extractable organic carbon and nutrient extraction procedure following Gregorich and Carter (2007, p. 651). This procedure was designed to minimize excessive physical disruption of sediment and release of dissolved organic carbon or nutrients that would have remained associated with the sediment under natural conditions instead of partitioning into the liquid phase, and to reflect the carbon and nutrient pools that would be available to microbes and roots. DI water extracts are generally thought to be more representative of porewater chemistry and yield lower concentrations of dissolved constituents compared to extraction solutions containing salt (typically 0.5 M $K_2SO_4$ or 2 M KCl) (Jones and Willett 2006; Mavi 2018). On the day following sediment collection, we applied the protocol by placing a 50 g field moist subsample of sediment and 500 mL of deionized water (18.2 MΩ) into a 12.7 × 20.32 cm low density polyethylene bag for 24 h. Following the extraction period, samples were filtered using Whatman® GF/F filters (0.7 $\mu$m) into glass test tubes in order to measure total dissolved nitrogen (TDN), nitrate ($NO_3$), soluble reactive phosphorus (SRP), total dissolved phosphorus (TDP), and total dissolved organic carbon (DOC). Samples for DOC were frozen at −80°C until analysis.

Samples for measurement of TDP were digested within 12–24 h by adding 0.2 g $K_2S_2O_8$ to each 20 mL filtered sample and then pressure cooking for 1 h to oxidize all reactive P to $PO_4^{3-}$. Samples were measured for SRP within 12–24 h of extraction. Both SRP and TDP were measured using a standard colorimetric method (Ostrofsky and Rigler 1987) using a Thermo Scientific GENESYS 10S UV–VIS Spectrophotometer (Waltham, Massachusetts, USA). Samples for measurement of TDN were also digested within 12–24 h by adding a solution of $K_2S_2O_8$ and NaOH and pressure cooking for 1 h to convert all nitrogen to nitrate (Solórzano and Sharp 1980). Both TDN and $NO_3$ samples were analyzed using the second-derivative method on the same spectrophotometer (Crumpton et al. 1992). DOC samples were analyzed using combustion on Apollo 9000 combustion TOC analyzer (Teledyne Tekmar Instruments, Mason, Ohio, USA) (Rice et al. 2018).

We measured mass loss-on-ignition (LOI) by allocating approximately 5 g of dried sediment to be burned at 550°C for 4 h in a muffle furnace. We estimated root biomass by wet sieving approximately half of the sediment remaining following the analyses described above. We wet-sieved by rehydrating sediment with 200 mL of tap water to catch particulates on the 1-mm sieve mesh. We

then picked and rinsed roots, dried them for 24 h at 60°C, and weighed them to obtain an estimate of root biomass for each core.

**Statistical analysis—overview, means, and estimates of season-long efflux**

We summarized sediment characteristics and $CO_2$ flux rates using a standard stratified means and variance calculation (Thomspon 2012). Strata corresponded with our nested sampling design in which collars were nested within transects, which were within ponds. Ponds were nested under hydroperiod classifications (i.e., temporary, semi-permanent, permanent). In addition to this analysis design matching our sampling design, we justified our decision to nest observations within this stratified organization by using ANOVA to test for differences in $CO_2$ flux at the various levels of organization (Supporting Information Table 2). All analyses were run in R (R Foundation for Statistical Computing 2017). Means are reported consistently throughout the paper as mean ± standard error (SE), unless otherwise noted.

In order to estimate the season-long efflux from exposed pond sediments, we expanded the analysis performed in DelVecchia et al. (2019), using the same methods, areal drying estimates, and $CO_2$ flux rates from water reported therein. For the subalpine sites, we simply revised the sediment $CO_2$ flux estimates to perform the same analysis as in DelVecchia et al. (2019). For the montane sites, we estimated a linear drying rate between pond being completely filled and completely dried, applied an estimate of total season length based on 5 years of prior data collected for M7 to all montane ponds, and thereby roughly estimated seasonal $CO_2$ flux for all ponds (*see* Supporting Information for more information).

**Statistical analysis—using principal components analysis to understand the effects of pond hydroperiod and drying time on sediment characteristics**

We used principal components analysis (PCA) to reduce dimensions of variance in sediment characteristics in order to (1) understand what variables characterized differences among sediment samples and (2) test whether two hydrologic variables (hydroperiod and earliest exposure date) could explain variance in principal coordinates that expressed the variance across all measured sediment characteristics. The PCA included all sediment characteristics measured: BD, LOI, pH, TOC, SRP, $NO_3$, TDN, root content, sediment temperature, and sediment moisture and was run separately for each the montane and the subalpine site.

We then used the coordinates on axes 1 and 2, which explained the largest fractions of variance in the data, as dependent variables in linear mixed effects models. We fit linear mixed effects models using the R package "nlme" (Pinheiro et al. 2014) and the maximum likelihood approach. We included as fixed effects the pond hydroperiod classification and the earliest exposure date. We included random effects for each pond, transect, and individual collar to test for the significance of the fixed effects. We ran the same models including only the pond as a random effect to test how much of the variation could be explained by unknown differences between each pond. We evaluated proportion of variance explained by the fixed and random effects by calculating pseudo *R*-squared values (R package MuMIn, Nakagawa and Schielzeth 2013).

**Statistical analysis—using linear mixed effects models to understand predictors of $CO_2$ flux rates**

The $CO_2$ flux rates were highly right skewed, with a Shapiro–Wilk $W$ value of 0.8983 ($n$ = 726, $p < 0.001$). Log-transforming the rates improved the normality of the distribution, but still yielded a significant $W$ value of 0.94252 ($p < 0.001$).

We used log-transformed flux rates to fit linear mixed effects models using a maximum likelihood approach. We used a random intercept effect structure in which individual collars were nested within transects, which were nested within ponds, to account for residual correlation structure in residuals at each level of organization. We used backwards elimination to begin with the most complex possible linear mixed-effects model, then remove variables one at a time based on which were not significant, evaluating the AIC (Akaike Information Criterion) score at each step of variable removal (Akaike 1998). We defined the best-fit linear model as the one that minimized the AIC score without removal of predictors that were significant in the ANOVA *F*-tests (Anderson and Burnham 2004). We included pseudo *R*-squared values to estimate variance explained by each model using the R package MuMIn (Nakagawa and Schielzeth 2013). We included both the marginal $R^2$ values that are based on fixed effects alone, and conditional $R^2$ values based on the combination of fixed and random effects. After a best-fit model was determined, we also removed each variable individually and examined the difference in pseudo *R*-squared values caused by each variable removal as an approach to understanding the explanatory power of various measurements.

We fit the models separately for each hydroperiod at the subalpine ponds, and for the ponds together at the montane site. We did so to compare which predictors were significant for each site and classification. We grouped all of the montane ponds because the semi-permanent ponds at the montane site are extremely similar to the temporary ponds in that the full surface area of the ponds dries in most years (they only remain wetted in one of 10 years) (SAW pers. obs.).

For each site and classification, we began with a base model that included the maximum possible explanatory variables. These base models included a continuous temporal autocorrelation function of the date that flux measurements were collected in each collar using R function corCAR1. Other independent variables included sediment moisture, temperature, LOI, date of flux rate measurement, earliest date of

sediment exposure (exposure date), extract pH, extract TOC, extract $NO_3$, extract TDN, extract SRP, extract TDP, root content, and sediment BD. We tested interactions between root biomass and all other variables, and sediment BD and LOI with other variables. We also tested for interactions between exposure date and date of measurement, which would be associated with the days between when a given collar became exposed and when the particular flux measurement was collected.

## Results

### Overall $CO_2$ flux rates and differences among pond hydroperiods and sites

Efflux rates differed significantly at every level of organization: within transects in the same pond, among ponds, among hydroperiods, and between the montane and subalpine sites (Table 1, Supporting Information Tables 1 and 2). Rates from exposed sediments at the montane site (stratified by transect and then by pond) averaged $331.5 \pm 111.5$ mmol $CO_2$ $m^{-2}$ $d^{-1}$. Within the montane site, rates were significantly higher in temporary ponds, which also tended to have higher LOI, higher SRP, and higher TDP (Fig. 3, Table 2). Semi-permanent ponds at the montane pond site dry approximately 9/10 years (SAW pers. obs.). Efflux rates from ponds at the subalpine sites were overall lower and averaged $142.8 \pm 45.1$ mmol $CO_2$ $m^{-2}$ $d^{-1}$. Notable differences among subalpine site pond hydroperiods included higher LOI in semi-permanent and temporary ponds but higher sediment moisture, TDN, SRP, and TDP in permanent ponds. Subalpine $CO_2$ flux rates were highest in the temporary and semi-permanent ponds, which differed significantly from the permanent ponds (Table 2). Although most sediment variables measured had similar ranges at the two sites, montane ponds tended to have higher pH values and lower LOI.

Scaling estimates of pond sediment $CO_2$ flux to the entire season length at each site showed that exposed pond sediments contributed an average of $30.8 \pm 6.0$ mol $m^{-2}$ $CO_2$ over a 162 d season at the montane site, and $6.1 \pm 2.3$ mol $m^{-2}$ $CO_2$ over the course of a 137–165 d season (depending on pond hydroperiod classification) at the subalpine site, consistent with montane ponds drying earlier than subalpine ponds and thus transitioning to exposed sediment $CO_2$ flux sooner. At the pond scale at the montane site, total efflux (water plus sediment efflux) was lowest in temporary ponds, with a mean of $25.2 \pm 20.0$ kmol $CO_2$ ($302.4 \pm 224.0$ kg C) per pond. It was highest in semi-permanent ponds, with a mean of $94.2 \pm 71.8$ kmol $CO_2$ ($1130.4 \pm 861.6$ kg C) per pond. At the subalpine site, total exposed sediment efflux had the lowest average of $1.6 \pm 0.6$ kmol $CO_2$ ($19.2 \pm 7.2$ kg C) per pond across the semi-permanent ponds, and the highest, $2.4 \pm 1.3$ kmol $CO_2$ ($28.8 \pm 15.6$ kg C) per pond and $8.6 \pm 3.4$ kmol $CO_2$ ($103.2 \pm 40.8$ kg C) per pond in the temporary ponds and permanent ponds, respectively. Season-long differences per pond were largely driven by pond area differences. Whereas, season-long efflux per $m^2$ decreased with pond permanence (temporary > semi-permanent > permanent; Supporting Information Table 4), further demonstrating the importance of drying and exposed sediment efflux. Including sediment $CO_2$ efflux estimates with $CO_2$ efflux from pond waters caused total pond efflux estimates to range from 1 to 17 times what might have been predicted if we had assumed pond areas were completely submerged over the course of the season and used only estimates of $CO_2$ flux from water (Supporting Information Fig. 5, Supporting Information Table 4).

### Sediment characteristics explained by pond, not by hydroperiod or exposure timing (Q. 1, 2)

We analyzed differences in the sediments at the montane and subalpine sites separately. At the montane site, PCA axes 1 and 2 combined could explain a total of 53% of the variance in sediment characteristics (Fig. 4, Supporting Information Table 3). Of this variance, root content, DOC, and LOI accounted for the most separation among sample points (i.e., individual collars). Sediment pH, SRP, TDP, and BD also accounted for larger fractions of the variance. When we used linear mixed effects models to test if pond hydroperiod or exposure date predicted sediment characteristics, we found that neither pond hydroperiod classification nor exposure date were significant (Table 3). The fixed effects of classification and exposure date explained a total of 3% of the variation in principal coordinate axis PC1 and 15% in PC2. The fixed and random effects of pond alone (not including the residual error structure of nested collars and transects) explained 74% of variation in PC1 and 58% in PC2 (Table 2). Similarly, we ran simple linear regressions of all variables vs. exposure date, but exposure date was not significant. Thus, the unknown differences among ponds explained much more of the variation in sediment characteristics than the exposure date or pond hydroperiod alone.

At the subalpine site, PCA axes 1 and 2 combined accounted for 52% of the variance in sediment characteristics among sample collars. Of this variance, sediment BD, moisture, root content, and LOI accounted for the most separation, while all other variables but sediment pH and temperature also appeared to account for some variation, especially between two ponds that were particularly different from the others (subalpine ponds 12 and 15). The linear mixed effects models showed that hydroperiod classification was a significant predictor of PC2 coordinates (ANOVA $F_{3,9} = 8.81$, $p = 0.0048$), but neither hydroperiod classification nor exposure day were significant in predicting PC1 coordinates. Overall, the fixed effects from the two models explained 9% of variation in PC1 and 41% in PC2. Using pond alone as a random variable explained 39% of the variation in PC1 and 58% of the variation in PC2. Similarly, using simple linear regressions of each variable vs. exposure date revealed significant negative relationships for roots and TOC and exposure date, but neither relationship explained more than 3% of the

**Table 1.** Mean ± SE values for a subset of variables measured at each pond and reference site along with pond metadata. Reference sites have only one sampling point each. Temperature refers to sediment temperature.

| Site | Classification | Pond | Area ($m^2$) | Tran sects | Collars | Bulk density (g $cm^{-3}$) | % loss-on-ignition | %moisture | Temperature (°C) | $CO_2$ efflux rate (mmol $m^{-2}$ $h^{-1}$) |
|---|---|---|---|---|---|---|---|---|---|---|
| Montane | Semi-permanent | M1 | 2040.1 | S, W, N | 8 | 0.51 ± 0.02 | 10.99 ± 0.48 | 41.88 | 19.09 | 5.23 ± 2.50 |
| Montane | Semi-permanent | M5 | 879.2 | S, W | 4 | 0.23 ± 0.01 | 40.72 ± 1.85 | 53.67 ± 12.83 | 27.44 ± 3.63 | 19.09 ± 6.36 |
| Montane | Semi-permanent | M6 | 1135.2 | S, W, N | 7 | 0.37 ± 0.01 | 19.63 ± 0.86 | 44.10 ± 8.00 | 26.37 ± 3.47 | 10.68 ± 7.04 |
| Montane | Semi-permanent | M7 | 318.0 | S, W | 5 | 0.33 ± 0.03 | 36.09 ± 5.22 | 45.74 ± 12.02 | 21.72 ± 7.53 | 10.22 ± 6.82 |
| Montane | Semi-permanent | M2 | 24,021.3 | S, W | 8 | 0.15 ± 0.01 | 61.38 ± 1.69 | 58.19 ± 9.48 | 26.29 ± 4.39 | 10.45 ± 5.68 |
| Montane | Temporary | M3 | 18.2 | S | 2 | 0.34 ± 0.03 | 21.33 ± 1.46 | 27.39 ± 10.43 | 25.78 ± 5.21 | 18.40 ± 14.09 |
| Montane | Temporary | M4 | 307.0 | W | 4 | 0.37 ± 0.00 | 27.49 ± 0.86 | 41.83 ± 13.30 | 28.37 ± 4.11 | 12.72 ± 5.45 |
| Montane | Temporary | M8 | 1172.0 | S, W | 4 | 0.28 ± 0.03 | 41.00 ± 5.62 | 32.09 ± 15.38 | 23.71 ± 6.33 | 23.86 ± 9.32 |
| Montane | Reference | | | | 1 | 0.42 | 15.25 | 7.8 ± 1.61 | 27.88 ± 6.46 | 13.63 ± 6.59 |
| Montane | Reference | | | | 1 | 0.48 | 14.91 | 10.25 ± 0.35 | 34.00 ± 0.28 | 19.09 ± 5.00 |
| Montane | Reference | | | | 1 | | 16.38 | 5.45 ± 2.12 | 30.55 ± 0.21 | 18.63 ± 12.72 |
| Subalpine | Permanent | S01 | 5199.1 | N, W | 7 | 0.13 ± 0.01 | 57.76 ± 1.24 | 60.89 ± 10.86 | 24.08 ± 3.23 | 2.95 ± 2.73 |
| Subalpine | Permanent | S03 | 183.3 | N, E | 8 | 0.10 ± 0.01 | 59.50 ± 2.01 | 63.25 ± 6.40 | 22.76 ± 3.92 | 5.23 ± 3.18 |
| Subalpine | Permanent | S05 | 1195 | S, E | 8 | 0.05 ± 0.00 | 52.72 ± 1.79 | 66.87 ± 3.30 | 17.75 ± 2.75 | 2.04 ± 2.04 |
| Subalpine | Permanent | S12 | 2013.2 | S, N | 9 | 0.11 ± 0.02 | 69.73 ± 1.11 | 57.26 ± 6.39 | 22.62 ± 3.69 | 5.91 ± 4.09 |
| Subalpine | Semi-permanent | S06 | 287.8 | N, W | 7 | 0.16 ± 0.02 | 62.61 ± 2.69 | 52.08 ± 8.11 | 20.94 ± 4.32 | 6.82 ± 2.95 |
| Subalpine | Semi-permanent | S08 | 993.5 | N, E | 8 | 0.35 ± 0.02 | 77.75 ± 1.83 | 39.50 ± 10.30 | 19.74 ± 4.41 | 3.86 ± 4.54 |
| Subalpine | Semi-permanent | S10 | 314.2 | S, E | 8 | 0.17 ± 0.02 | 69.47 ± 3.65 | 52.54 ± 7.51 | 20.64 ± 3.62 | 7.27 ± 2.04 |
| Subalpine | Semi-permanent | S44 | 224.6 | S, N | 9 | 0.09 ± 0.01 | 59.98 ± 2.33 | 59.39 ± 12.81 | 24.64 ± 7.03 | 8.41 ± 5.00 |
| Subalpine | Temporary | S13 | 90.5 | N, W | 7 | 0.18 ± 0.01 | 77.72 ± 1.21 | 47.34 ± 9.47 | 22.56 ± 5.13 | 6.36 ± 4.54 |
| Subalpine | Temporary | S15 | 81.2 | N, E | 8 | 0.16 ± 0.02 | 60.29 ± 2.33 | 34.45 ± 11.60 | 20.27 ± 3.93 | 5.00 ± 2.73 |
| Subalpine | Temporary | S22 | 231.3 | S, E | 8 | 0.21 ± 0.01 | 63.67 ± 3.68 | 31.78 ± 16.35 | 22.70 ± 4.17 | 10.00 ± 3.41 |
| Subalpine | Temporary | S42 | 118.3 | S, N | 9 | 0.31 ± 0.01 | 59.51 ± 1.37 | 37.85 ± 7.74 | 25.09 ± 4.28 | 7.50 ± 2.04 |
| Subalpine | Reference | | | | 1 | 0.41 | 70.81 | 3.64 ± 3.97 | 28.13 ± 2.87 | 19.09 ± 6.82 |
| Subalpine | Reference | | | | 1 | | 77.05 | 6.02 ± 4.57 | 24.00 ± 3.02 | 7.27 ± 2.04 |
| Subalpine | Reference | | | | 1 | 0.27 | 85.32 | 13.00 | 21.30 ± 8.57 | 7.50 ± 2.95 |

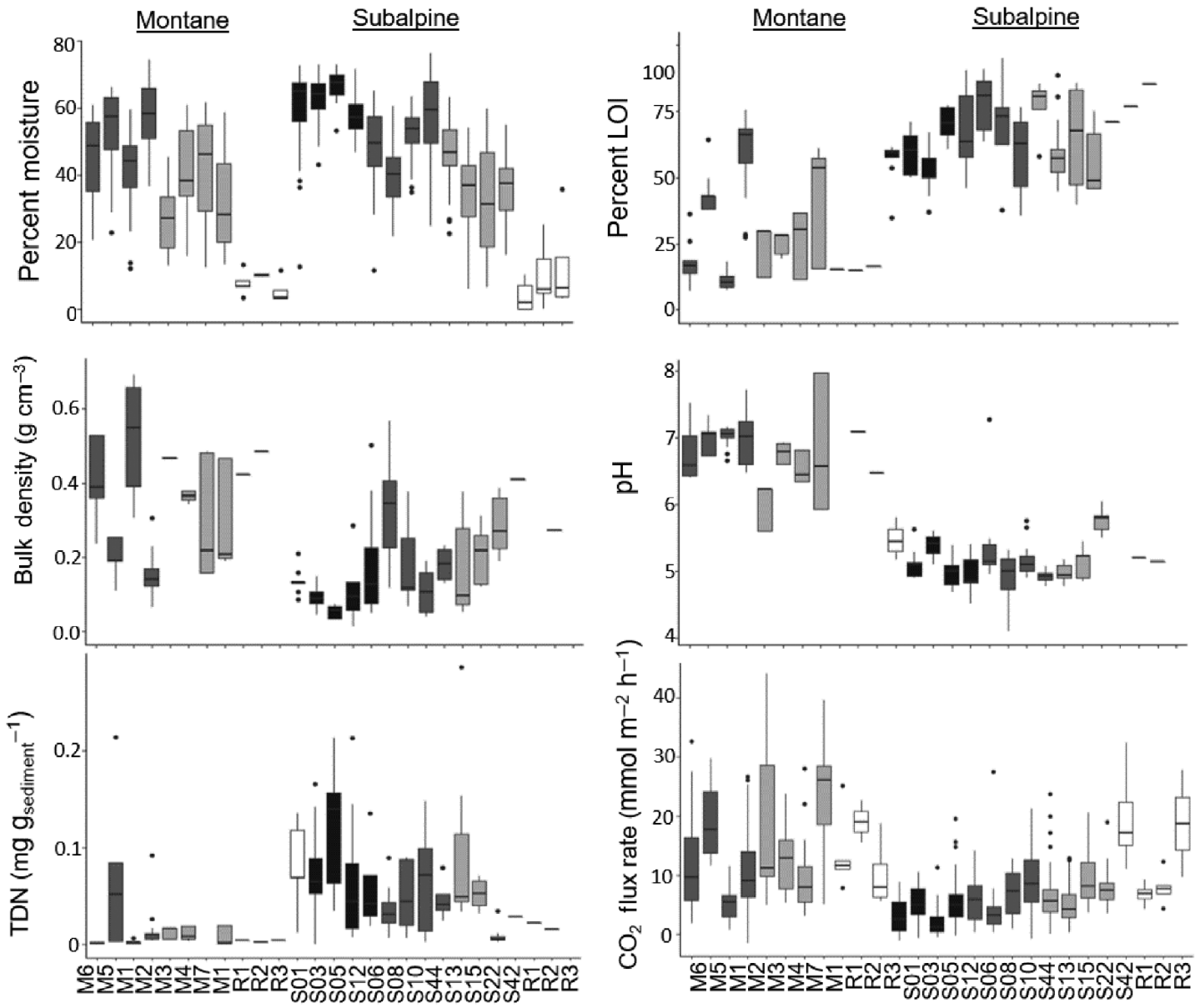



**Fig 3.** Boxplots of all collar measurements from each pond (line represents median, boxes represent interquartile range, dots represent outliers). Dark fills are permanent ponds; medium fills are semi-permanent ponds, light points are temporary ponds, and white fills or single measurements are reference sites. Additional data are shown in Supporting Information Fig. 3, and summary statistics are reported in Table 1. Flux rate refers to $CO_2$ flux rate.

variance. Similar to montane sites, the random differences among ponds explained far more variation than the exposure date or hydroperiod classification.

### Variation in sediment $CO_2$ flux rates was explained by sediment characteristics (Q. 3)

The fixed effects of all best-fit models (all montane ponds, and each hydroperiod classification at the subalpine ponds) explained 46–57% of the variation in $CO_2$ flux rates, whereas the combined fixed and random effects explained 59–70% of the variation in $CO_2$ flux rates across models (values reported in Table 4). All best-fit models included a significant interaction term between sediment moisture and sediment temperature (Table 5). All best fit models also included BD and TOC. In the semi-permanent subalpine ponds, the removal of temperature from the best-fit model had the greatest effect (of any variable removal from that model) on the marginal $R^2$ value, causing a decrease from 0.57 to 0.42 (Table 6).

An interaction between BD and LOI (which could reflect compressed organic-matter rich sediments vs. heavier mineral sediments) was a significant predictor in the montane ponds and in the permanent subalpine ponds, and similarly, the interaction between BD and TOC was significant in the temporary subalpine ponds. In the montane ponds, the removal of BD

**Table 2.** Mean ± SE values for each variable by hydroperiod and site. * indicates that $NO_3$ and TDN units are in units of $\mu g\ g^{-1}$ (dry sediment) for montane ponds and $mg\ g^{-1}$ (dry sediment) for subalpine ponds.

| Site | Classification | Bulk density ($g\ cm^{-3}$) | % loss-on-ignition | TOC ($mg\ g^{-1}$) | pH | SRP ($\mu g\ g^{-1}$) | TDP ($\mu g\ g^{-1}$) | $NO_3$ ($mg\ g^{-1}$) | TDN (*$g\ g^{-1}$) | Roots ($mg\ g^{-1}$) | $CO_2$ efflux rate ($mmol\ m^2\ h^{-1}$) | % moisture | Temperature (°C) |
|---|---|---|---|---|---|---|---|---|---|---|---|---|---|
| Montane | Semi-permanent | 0.30 ± 0.02 | 15.51 ± 2.83 | 0.07 ± 0.00 | 6.87 ± 0.03 | 0.57 ± 0.11 | 0.79 ± 0.04 | 0.00 ± 0.00 | 0.03 ± 0.00 | 7.46 ± 0.00 | 11.13 ± 1.14 | 40.54 ± 2.57 | 25.92 ± 0.97 |
| Montane | Temporary | 0.23 ± 0.01 | 27.64 ± 7.00 | 0.20 ± 0.03 | 6.44 ± 0.12 | 2.54 ± 0.06 | 1.26 ± 0.03 | 0.00 ± 0.00 | 0.01 ± 0.00 | 9.57 ± 0.04 | 18.18 ± 2.50 | 33.68 ± 3.24 | 25.98 ± 1.34 |
| Subalpine | Permanent | 0.09 ± 0.01 | 58.71 ± 2.01 | 0.11 ± 0.00 | 5.27 ± 0.02 | 0.56 ± 0.05 | 2.26 ± 1.46 | 0.01 ± 0.53 | 0.09 ± 0.00 | 12.8 ± 0.01 | 4.09 ± 0.45 | 61.77 ± 1.43 | 22.15 ± 0.86 |
| Subalpine | Semi-permanent | 0.20 ± 0.03 | 68.50 ± 2.99 | 0.11 ± 0.00 | 5.11 ± 0.04 | 0.30 ± 0.05 | 1.60 ± 0.22 | 0.00 ± 0.15 | 0.05 ± 0.00 | 8.13 ± 0.00 | 6.36 ± 0.68 | 49.71 ± 1.53 | 21.34 ± 0.69 |
| Subalpine | Temporary | 0.22 ± 0.01 | 65.89 ± 3.50 | 0.10 ± 0.00 | 5.19 ± 0.01 | 0.35 ± 0.02 | 1.36 ± 0.23 | 0.02 ± 0.21 | 0.05 ± 0.00 | 3.37 ± 0.00 | 7.04 ± 0.45 | 37.16 ± 1.56 | 22.69 ± 0.57 |
| Montane | Reference | 0.45 | 15.51 | 0.07 | 6.77 | 0.57 ± 0.01 | 0.64 | 0.00 ± 0.01 | 0.00 | 7.24 ± 0.01 | 12.27 ± 1.59 | 6.80 ± 1.07 | 18.00 ± 1.93 |
| Subalpine | Reference | 0.34 | 77.72 | 0.02 | 5.17 | 0.12 ± 0.01 | 0.37 | 0.00 ± 0.01 | 0.02 | 0.75 ± 0.01 | 6.59 ± 1.36 | 45.71 ± 4.17 | 22.93 ± 1.35 |

from the best fit model caused a decrease in the marginal pseudo $R^2$ value from 0.53 to 0.33, whereas removal of any other variable from that best-fit model caused decreases of 0–0.07.

TOC was included in all best-fit models, but significant only in the subalpine ponds. LOI was included in best-fit models for semi-permanent subalpine ponds as well. Sediment pH was included in all best-fit models except the semi-permanent subalpine ponds. In the temporary subalpine ponds, removal of pH from the best-fit model reported caused the largest decrease (of any other variable included in that model) in the marginal pseudo $R^2$ value from 0.45 to 0.36, which was the same as the change caused by removal of temperature, which yielded a marginal $R^2$ value of 0.36 (removal of both yielded a value of 0.28).

Root biomass (roots) was not included in best-fit models for semi-permanent or temporary subalpine ponds, but it was included independently and as an interaction with nutrient pools in the permanent subalpine ponds and independently in the montane ponds. In the permanent subalpine ponds, roots interacted with $NO_3$, TDN, TOC, and TDP. Removal of roots as an explanatory variable (including all interactions) from the best-fit model in this classification caused a drop in the marginal pseudo $R^2$ of 0.04. However, removal of $NO_3$ and the $NO_3$ x roots interaction caused the largest decrease in the marginal pseudo $R^2$ value from 0.52 in the best fit model to 0.44 in the nitrate removed model. Similarly, removal of TDP and TDP x roots caused a decrease from 0.52 to 0.47. Therefore, in the permanent subalpine ponds model, extract nutrient content and the interactions between extract nutrient content and root biomass had more explanatory power than root biomass alone, or any other variable included in the model. In the montane pond best-fit models, removal of roots from the best fit model caused a minor decrease in the marginal pseudo $R^2$ from 0.53 to 0.52, and in the conditional pseudo $R^2$ from 0.59 to 0.58.

Exposure date was included in all best-fit models except the temporary subalpine ponds. The exposure date and measurement date interaction, representative of days since a given collar was exposed to air, was not included in any of the best fit models. The best fit models for the temporary subalpine ponds and the montane ponds included a continuous autocorrelation function as a function of date. Examination of autocorrelation plots showed that correlations were significant at a lag time of 2 d in the temporary subalpine ponds, and 1 and 2 d in the montane ponds.

## Discussion

In this study, we found that exposed sediments in ponds had $CO_2$ efflux rates that were an order of magnitude higher than previously published estimates from pond waters. Efflux rates from sediments at the montane site (333.7 ± 43.8 mmol $CO_2\ m^{-2}\ d^{-1}$) and from ponds at the subalpine sites (140.1 ± 14.9 mmol $CO_2\ m^{-2}\ d^{-1}$) were approximately 10–33 times greater than the global average of 35.2 ± 14.9 mmol $CO_2\ m^{-2}\ d^{-1}$ for efflux from water in ponds < 0.001 $km^2$ (Holgerson and Raymond 2016). The exposed sediment efflux rates were also an order of magnitude

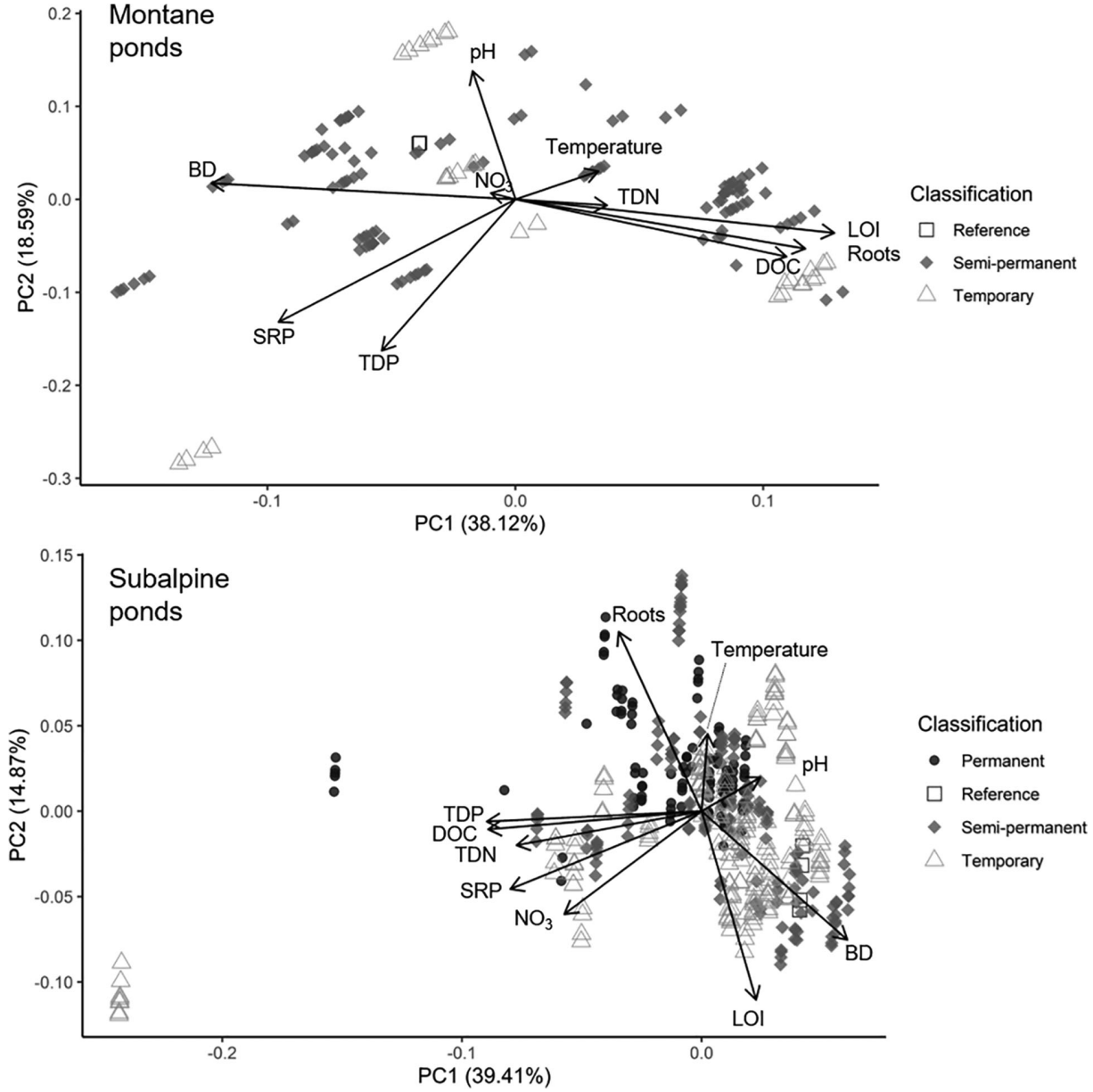



**Fig 4.** A PCA of pond sediment properties at each site was used to reduce dimensions of variance and test for the effects of pond hydroperiod classifications and sites. Data points are soil characteristics within each collar.

higher than the $CO_2$ efflux rate measured from waters of the subalpine ponds in 2017, $10.7 \pm 10.2$ mmol $CO_2$ $m^{-2}$ $d^{-1}$ (DelVecchia et al. 2019). Scaling these rates to entire ponds over the course of the 2018 season showed that accounting for pond sediment $CO_2$ efflux could raise season-long $CO_2$ flux estimates in these systems by 1–17 times. Ponds of varying hydroperiods had significantly different sizes and area-specific flux over the course of a season, so scaling to entire pond areas involved a clear interplay between pond areas and tendency to dry down (Supporting Information Table 2). These high flux rates from exposed pond sediments are consistent with site-specific studies that have considered exposed pond sediments (Catalán et al. 2014; Obrador et al. 2018) and in range of recently globally-compiled rates of pond sediment $CO_2$ flux, which had a mean of $267 \pm 221$ mmol $m^{-2}$ $d^{-1}$ (mean ± SD, Keller et al. 2020).

Although measuring $CO_2$ fluxes from sediments without measuring primary productivity can lead to an overestimate of overall flux, vegetation in the collar locations was very minimal and evidenced by low root content in the samples. Furthermore, sediments with high root content can also have higher overall flux rates as a result of autotrophic respiration contributions but roots did not have consistent or significant influences on best-fit models across locations, suggesting that other drivers (heterotrophic respiration) might be more important at these sites.

**Table 3.** *F*-test statistics and pseudo *R*-squared values are reported for the linear mixed effects models used to test the fixed effects of pond classification and collar exposure date on PCA coordinates with random effects of collars nested within transects, nested within ponds.

| Site | Axis | Variable | df | *F* | *p* |
|---|---|---|---|---|---|
| Subalpine | PC1 | Classification | 3, 9 | 1.334 | 0.32 |
| Subalpine | PC1 | Day | 1, 70 | 0.777 | 0.38 |
| Subalpine | PC2 | Classification | 3, 9 | 8.817 | 0.005 |
| Subalpine | PC2 | Day | 1, 70 | 0.712 | 0.40 |
| Montane | PC1 | Classification | 2, 5 | 0.279 | 0.77 |
| Montane | PC1 | Day | 1, 19 | 0.298 | 0.59 |
| Montane | PC2 | Classification | 2, 5 | 2.168 | 0.21 |
| Montane | PC2 | Day | 1, 19 | 1.042 | 0.32 |

| Site | Axis | Variance explained (%) | Marginal $R^2$ | Conditional $R^2$ | Var. expl. × Marg. $R^2$ (%) | Cond. $R^2$ (ponds only) |
|---|---|---|---|---|---|---|
| Subalpine | PC1 | 35.9 | 0.09 | 0.99 | 3.2 | 0.39 |
| Subalpine | PC2 | 16.3 | 0.41 | 0.93 | 6.6 | 0.58 |
| Montane | PC1 | 36 | 0.03 | 0.99 | <1 | 0.74 |
| Montane | PC2 | 17 | 0.15 | 0.99 | 5.4 | 0.58 |

**How do sediment characteristics relate to pond hydroperiod and timing of exposure (Q. 1, 2)?**

Our first questions asked if sediment characteristics related to pond hydroperiods and the timing of exposure. Overall, sediment characteristics did not differ by hydroperiod classification or the earliest exposure date from 2018. The exception to this was at the subalpine site, where the exposure date was a significant predictor of axis PC2 coordinates. Hydrologic history, or the historical frequency and duration of drying, can create distinct microbial habitats constrained by pH and organic matter properties (Reverey et al. 2018). Indeed, the subalpine site had more of a gradient of pond drying than the montane site, which might have created more variation in sediment conditions. Root content (positively correlated) and BD (negatively correlated) were the top two loadings into this axis, suggesting that the earlier a given sediment segment dried, the more likely it was to have higher root content and lower BD, consistent with the potential for plant encroachment (Nitzsche et al. 2017) Although sedge in the ponds was very limited (mostly *Carex aquatilis*), we also observed that it occurred more frequently at pond margins.

Regardless, pond hydroperiod and exposure date alone did not account for large amounts of variation in aggregate or individual sediment characteristics at any site, explaining < 7% of the variation on any principal component axis used. However, including a random effect structure for the pond itself explained up to 74% of the variance. Although we measured exposure date for each sediment sample in 1 year, we would expect the relative differences between earliest exposure dates to remain constant between years because collars were placed increasingly closer to the centers of ponds. Thus, 2018 results likely reflect relationships that might exist generally at these pond sites. Our finding that pond sediment characteristics were not predicted by a legacy

**Table 4.** Best fit models, fit statistics, and variance explained for each pond hydroperiod/site. cont. ACF indicates that the continuous autocorrelation function was included in the best fit model. AIC scores also indicate change from base model AIC.

| Classification | Permanent | Semi-permanent | Temporary | Montane (all temp) |
|---|---|---|---|---|
| Fixed effect structure | Temp × moist + BD × LOI + pH + TDP × roots + TOC × roots + $NO_3$ × roots + TDN × roots + exposure | Temp × moist + date + BD + LOI + TOC + SRP + exposure | Temp × moist + date + BD × TOC + pH + cont. ACF | Temp × moist + date + BD × LOI + BD × TOC + pH + SRP + roots + exposure + cont. ACF |
| *n* | 114 | 162 | 191 | 146 |
| AIC (difference from base model AIC) | 238.96 (– 9.34) | 196.1 (– 17.10) | 103.91 (– 16.56) | 222.97 (– 11.03) |
| BIC | 296.42 | 239.3 | 146.19 | 282.64 |
| Log likelihood | –98.48 | –84.04 | –38.96 | –91.49 |
| $R^2$ marginal | 0.52 | 0.57 | 0.46 | 0.53 |
| $R^2$ conditional | 0.70 | 0.65 | 0.66 | 0.59 |

**Table 5.** Coefficients, *F* statistics, (degrees of freedom) *F* values, and *p* values are listed for each best-fit model of the PCA coordinates obtained from the analyses presented in Fig. 3.

| Predictor | Perm | *F* stat, *F*, *p* | Semi-perm | *F* stat, *F*, *p* | Temporary | *F* stat, *F*, *p* | Kettle | *F* stat, *F*, *p* |
|---|---|---|---|---|---|---|---|---|
| Intercept | 606.411 | (1109) 100.8, < 0.0001 | 344.530 | (1121) 463.8, <0.0001 | 84.132 | (1156) 82.69, <0.0001 | 38.123 | (1109) 117.00, <0.0001 |
| Temp. | 0.303 | (1.109) 13.86. 0.0003 | 0.125 | (1121) 64.96, <0.0001 | −0.042 | (1156) 49.74, <0.0001 | 0.048 | (1109) 14.70, 0.0002 |
| Moisture | 0.066 | (1109) 12.67, 0.0006 | 0.035 | (1121) 0.28, 0.599 | −0.041 | (1156) 9.28, 0.003 | 0.003 | (1109) 13.47, 0.0004 |
| Moist : Temp | −0.005 | (1109) 2.16, 0.144 | −0.0014 | (1121) 4.21, 0.042 | 0.002 | (1156) 54.77, <0.0001 | −0.001 | (1109) 2.15, 0.146 |
| BD | −41.536 | (1,8) 10.52, 0.012 | 0.138 | (1,25) 8.11, 0.009 | | | −1.731 | (1,10) 11.94, 0.006 |
| LOI | −0.074 | (1,8) 4.94, 0.057 | −0.003 | (1,25) 4.19, 0.051 | | | 0.003 | (1,10) 4.62, 0.057 |
| pH | −0.020 | (1,8) 3.86, 0.085 | | | 0.439 | (1,20) 3.65, 0.071 | 0.050 | (1,10) 5.11, 0.047 |
| SRP | | | −0.123 | (1,25) 3.34, 0.080 | | | | |
| TDP | 0.371 | (1,8) 1.95, 0.199 | | | | | 0.238 | (1,10) 2.26, 0.163 |
| $NO_3$ | | | | | | | | |
| TDN | | | | | | | | |
| Roots | −0.623 | (1,8) 5.50, 0.047 | | | | | 2.481 | (1,10) 10.13, 0.010 |
| Roots : TDP | −46.467 | (1,8) 0.45, 0.52 | | | | | 17.858 | (1,10) 1.24, 0.292 |
| TOC | −4.225 | (1,8) 6.18, 0.037 | 1.204 | (1,25) 25.86, <0.0001 | −0.023 | (1,20) 13.69, 0.001 | −6.264 | (1,10) 2.00, 0.188 |
| Exposure | −0.034 | (1,8) 2.74, 0.136 | −0.019 | (1,25) 22.86, 0.0001 | | | −0.002 | (1,10) 3.03, 0.113 |
| Roots : TOC | 1047.644 | (1,8) 0.33, 0.581 | | | | | | |
| Roots : TDN | 278.771 | (1,8) 0.19, 0.676 | | | | | | |
| Roots : $NO_3$ | −5251.488 | (1,8) 0.69, 0.429 | | | | | | |
| BD : LOI | 0.655 | (1,8) 11.57, 0.009 | | | | | 0.080 | (1,10) 12.69, 0.005 |
| Date | | | | | −0.005 | (1156) 24.54, <0.0001 | | |
| BD : TOC | | | | | 22.519 | (1,20) 6.02, 0.023 | 23.050 | (1,10) 1.96, 0.192 |

**Table 6.** Pseudo *R*-squared values are reported for the best-fit models compared to the best fit models with each individual listed variable removed show the variance explained by inclusion of each variable.

| | Perm | | Semi-perm | | Temporary | | Montane | |
|---|---|---|---|---|---|---|---|---|
| Predictor | Marg. $R^2$ | Cond. $R^2$ | Marg. $R^2$ | Cond. $R^2$ | Marg. $R^2$ | Cond. $R^2$ | Marg. $R^2$ | Cond. $R^2$ |
| Best-fit model | 0.52 | 0.71 | 0.57 | 0.65 | 0.45 | 0.66 | 0.53 | 0.59 |
| Temp. | 0.49 | 0.70 | **0.42** | **0.59** | **0.36** | **0.63** | 0.48 | 0.70 |
| Moisture | 0.49 | 0.69 | 0.53 | 0.62 | | | 0.51 | 0.57 |
| BD | 0.51 | 0.61 | 0.57 | 0.65 | 0.41 | 0.56 | **0.33** | **0.57** |
| LOI | 0.48 | 0.64 | 0.55 | 0.65 | | | 0.52 | 0.59 |
| pH | 0.52 | 0.71 | | | **0.36** | **0.60** | 0.53 | 0.59 |
| SRP | | | 0.55 | 0.65 | | | 0.50 | 0.58 |
| TDP | 0.47 | 0.63 | | | | | 0.46 | 0.56 |
| $NO_3$ | **0.44** | **0.65** | | | | | | |
| TDN | | | | | | | | |
| Roots | 0.49 | 0.62 | | | | | 0.52 | 0.58 |
| TOC | 0.50 | 0.63 | 0.49 | 0.64 | 0.39 | 0.53 | 0.50 | 0.61 |
| Exposure | 0.55 | 0.64 | 0.51 | 0.66 | | | 0.53 | 0.59 |
| Date | | | 0.57 | 0.65 | | | 0.53 | 0.58 |

Bold values indicate variables for which removal from the best-fit model caused the greatest decrease in the $R^2$ value.

of sediment inundation and exposure (hydroperiod) or the timing of exposure in the study year was unexpected, and highlighted the heterogeneity among ponds even in a close proximity that we otherwise expected would be somewhat similar.

Although our approach using PCA to reduce dimensions of sediment characteristics did not show an effect of exposure date, the exposure date was included in most best-fit models of sediment $CO_2$ flux rates, even though these models already included the sediment moisture which decreased over the time that pond sediments were exposed. The only best-fit model which did not include the exposure date as a predictor was that of the temporary subalpine ponds. It is likely that exposure date was not a predictor of flux in these ponds because they tended to have flat basin shapes and smaller sizes, so exposure dates were more uniform across the pond and thus not as useful for characterizing variation.

### How do sediment $CO_2$ flux rates relate to sediment characteristics?

Our third question asked how sediment $CO_2$ flux related to sediment characteristics. Although sediment $CO_2$ efflux rates have been shown in multiple instances to far exceed water efflux rates (Catalán et al. 2014; Obrador et al. 2018; DelVecchia et al. 2019), inclusions of small lentic water bodies in carbon accounting are still based on water flux rate estimates alone (Holgerson and Raymond 2016). Furthermore, our understanding of environmental controls on $CO_2$ efflux from exposed aquatic sediments includes complex relationships with sediment moisture, temperature, and organic matter content, but these relationships are geographically limited and lack information on how extractable dissolved nutrient content and sediment properties could affect $CO_2$ flux rates (Marcé et al. 2019).

The fixed effects alone (sediment characteristics variables) which we considered in sediment $CO_2$ flux best-fit models explained 46–57% of the variation in flux rates depending on site and hydroperiod, whereas the inclusion of ponds, transects, and locations along transects contributed to explaining an additional 8–20% of the variance in each model. Therefore, the sediment characteristics that we measured seem to have encompassed much of the spatial variation between individual sediment sampling locations across ponds at each site/hydroperiod classification.

Best-fit models consistently included an interaction term between sediment temperature and moisture, as expected given known temperature and moisture controls on both heterotrophic and autotrophic respiration. We do, however, note that we specifically structured our sampling to consider sediment moisture at times not immediately after rainfall, not only because our instruments could not function in rainy conditions but because rainfall, or any sediment rewetting, can cause temporary pulses of $CO_2$ from sediments due to displacement of gases from sediment pore spaces (Gallo et al. 2014) as well as enhanced decomposition (Birch 1959; Jarvis et al. 2007). Therefore, our estimates of $CO_2$ flux rates could have led to underestimates of $CO_2$ flux over the season, because we did not measure short-term pulses after rainfall or rewetting.

Other than sediment moisture and temperature, extractable dissolved organic carbon was the only variable included in all best-fit models. These findings were similar to those of Obrador et al. (2018) from exposed Mediterranean pond sediments, in which organic matter content, temperature, and humidity were predictors of $CO_2$ flux. Other studies which have considered $CO_2$ flux from exposed aquatic sediments have also found that other than sediment moisture and temperature, organic carbon content is a significant predictor of $CO_2$ flux (Gallo et al. 2014).

Sediment pH is not a commonly studied predictor of flux (e.g., Marcé et al. 2019). Although pH was included in best-fit models from all but the semi-permanent subalpine ponds, it only appeared to explain variation in flux rates in the temporary subalpine ponds, where removal of pH from the best fit model caused a decrease in the marginal $R^2$ of 0.09, more than any other variable in the model. Given the lack of root content in the best-fit model, we might conclude that in this particular context, pH was a driver of microbial processes. Indeed pH explains 70% of variation in sediment bacterial diversity globally (Fierer and Jackson 2006). Lower pH is associated with higher dominance of fungal biomass over bacterial biomass and lower respiration rates in terrestrial sediments (Rousk et al. 2009), and lower $CO_2$ efflux rates in freshwater peatland and swamp sediments (Bridgham and Richardson 1992).

Similarly, BD, LOI values, interactions between BD and LOI, and interactions between BD and TOC were included in several but not all best-fit models. These were factors, along with pH, which differed between the subalpine and montane pond clusters, suggesting a potential broader geographical scale difference between $CO_2$ flux rates, such as from underlying geology, surrounding vegetation types, elevation, or another difference between the two sites. BD explained the most variation in the montane best-fit model (20%), suggesting that underlying geology and compaction could have a particularly large effect on $CO_2$ flux rates in some locations. In contrast to the subalpine site, BD and LOI were negatively correlated at the montane site, suggesting that higher BD corresponded to higher inorganic sediment composition. The subalpine ponds, consistent with their lower BD values, lower pH values, and higher LOI values, were located in a landscape area that was peat rich and spruce-dominated. If these organic matter sources influenced or were included in pond sediments, they could become more compacted over time. The permanent subalpine pond best-fit models included an interaction term between BD and LOI that could suggest compaction of organic matter. BD and LOI can also relate to sediment aeration and oxygen supply, as well as the ability for water to displace gases (Gallo et al. 2014).

Extractable TOC reflected the amount of TOC available for microbial respiration, but it also was related to LOI and BD, even though those measures reflect bulk properties of the sediment rather than what is extractable. The best-fit model for the temporary subalpine ponds did not include BD or LOI individually, but only an interaction term between BD and TOC. Perhaps denser sediments reflected some compaction of organic materials from which TOC was still extractable.

## Conclusion

Our results showed a site-specific and potentially hydroperiod-specific difference in the drivers of $CO_2$ flux (Question 3), even though sediment characteristics themselves did not consistently differ among hydroperiods (Question 1). Variables such as temperature, moisture, and organic matter content are recognized as drivers of exposed aquatic sediment $CO_2$ flux in sites studied thus far (Marcé et al. 2019) but our data showed that extractable nutrient content and pH can be important explanatory variables in particular contexts. In contrast to what we expected, the timing of sediment exposure was neither a predictor of sediment characteristics nor a consistent or powerful predictor of $CO_2$ flux rates, although hydrology still affected $CO_2$ flux rates simply by affecting sediment moisture and the timing of when sediments switch from submerged to exposed (DelVecchia et al. 2019). Overall, the variables we measured explained 46–57% of variation in $CO_2$ flux rates and an additional 6–18% of variation could be explained by unmeasured differences among ponds. Our results stress the importance of local context in determining drivers of $CO_2$ flux as aquatic sediments become exposed over time and at a higher frequency and longer duration as climate change increases warming, decreases snowpack, and shifts precipitation especially at higher elevations.

## References

Akaike, H. 1998. Information theory and an extension of the maximum likelihood principle, p. 199–213. *In* Selected papers of Hirotugu Akaike. Springer.

Anderson, D. R., and K. Burnham. 2004. Model selection and multi-model inference. Second. Springer-Verlag.

Arnell, N. W. 1999. Climate change and global water resources. Glob. Environ. Chang. **9**: S31–S49.

Barnett T. P., J. C. Adam, and D. P. Lettenmaier. 2005. Potential impacts of a warming climate on water availability in snow-dominated regions. Nature **438**: 303–309. doi:10.1038/nature04141

Batzer, D. P., R. B. Rader, and S. A. Wissinger. 1999. Invertebrates in freshwater wetlands of North America: Ecology and management. John Wiley & Sons.

Birch, H. F. 1959. Further observations on humus decomposition and nitrification. Plant Soil **11**: 262–286. doi:10.1007/BF01435157

Boone, R. D., K. J. Nadelhoffer, J. D. Canary, and J. P. Kaye. 1998. Roots exert a strong influence on the temperature sensitivity of soil respiration. Nature **396**: 570–572. doi:10.1038/25119

Bridgham, S. D., and C. J. Richardson. 1992. Mechanisms controlling soil respiration ($CO_2$ and $CH_4$) in southern peatlands. Soil Biol. Biochem. **24**: 1089–1099. doi:10.1016/0038-0717(92)90058-6

Burkett, V., and J. Kusler. 2000. Climate change: Potential impacts and interactions in wetlands of the United States. JAWRA J. Am. Water Resour. Assoc. **36**: 313–320. doi:10.1111/j.1752-1688.2000.tb04270.x

Carpenter S. R., S. G. Fisher, N. B. Grimm, and J. F. Kitchell 1992. Global Change and Freshwater Ecosystems. Annual Review of Ecology and Systematics **23**: 119–139. doi:10.1146/annurev.es.23.110192.001003

Catalán N., D. von Schiller, R. Marcé, M. Koschorreck, L. Gomez-Gener, and B. Obrador. 2014. Carbon dioxide efflux during the flooding phase of temporary ponds. Limnetica **33**: 349–360.

Cleveland C. C., D. R. Nemergut, S. K. Schmidt, and A. R. Townsend 2007. Increases in soil respiration following labile carbon additions linked to rapid shifts in soil microbial community composition. Biogeochemistry **82**: 229–240. doi:10.1007/s10533-006-9065-z

Clow D. W. 2010. Changes in the timing of snowmelt and streamflow in Colorado: A response to recent warming. J. Clim. **23**: 2293–2306.

Cole J. J., and others. 2007. Plumbing the Global Carbon Cycle: Integrating Inland Waters into the Terrestrial Carbon Budget. Ecosystems **10**: 172–185. http://dx.doi.org/10.1007/s10021-006-9013-8

Crumpton W. G., T. M. Isenhart, and P. D. Mitchell 1992. Nitrate and organic N analyses with second-derivative spectroscopy. Limnology and Oceanography **37**: 907–913. doi:10.4319/lo.1992.37.4.0907

Davidson, E. A., E. Belk, and R. D. Boone. 1998. Soil water content and temperature as independent or confounded factors controlling soil respiration in a temperate mixed hardwood forest. Glob. Chang. Biol. **4**: 217–227. doi:10.1046/j.1365-2486.1998.00128.x

DelVecchia, A. G., J. A. Balik, S. K. Campbell, B. W. Taylor, D. C. West, and S. A. Wissinger. 2019. Carbon dioxide concentrations and efflux from permanent, semi-permanent, and temporary subalpine ponds. Wetlands **39**: 955–969. doi:10.1007/s13157-019-01140-3

Downing, J. A., and others. 2006. The global abundance and size distribution of lakes, ponds, and impoundments. Limnol. Oceanogr. **51**: 2388–2397. doi:10.4319/lo.2006.51.5.2388

Duarte, C. M., and Y. T. Prairie. 2005. Prevalence of heterotrophy and atmospheric $CO_2$ emissions from aquatic ecosystems. Ecosystems **8**: 862–870. doi:10.1007/s10021-005-0177-4

Fang, C., and J. B. Moncrieff. 2001. The dependence of soil $CO_2$ efflux on temperature. Soil Biol. Biochem. **33**: 155–165. doi:10.1016/S0038-0717(00)00125-5

Fierer, N., and R. B. Jackson. 2006. The diversity and biogeography of soil bacterial communities. Proc. Natl. Acad. Sci. **103**: 626–631. doi:10.1073/pnas.0507535103

Fierer, N., and J. P. Schimel. 2003. A proposed mechanism for the pulse in carbon dioxide production commonly observed following the rapid rewetting of a dry soil. Soil Sci. Soc. Am. J. **67**: 798. doi:10.2136/sssaj2003.0798

Fromin, N., and others. 2010. Impact of seasonal sediment desiccation and rewetting on microbial processes involved in greenhouse gas emissions. Ecohydrology **3**: 339–348.

Gallo, E. L., K. A. Lohse, C. M. Ferlin, T. Meixner, and P. D. Brooks. 2014. Physical and biological controls on trace gas fluxes in semi-arid urban ephemeral waterways. Biogeochemistry **121**: 189–207. doi:10.1007/s10533-013-9927-0

Gómez-Gener, L., and others. 2016. When water vanishes: Magnitude and regulation of carbon dioxide emissions from dry temporary streams. Ecosystems **19**: 710–723. doi:10.1007/s10021-016-9963-4

Gregorich, E. G., and M. R. Carter. 2007. Soil sampling and methods of analysis. CRC Press. DOI: 10.1038/ngeo2654

Holgerson, M. A., and P. A. Raymond. 2016. Large contribution to inland water $CO_2$ and $CH_4$ emissions from very small ponds. Nat. Geosci. **9**: 222–226. doi:10.1038/ngeo2654

Iqbal, J., R. Hu, M. Feng, S. Lin, S. Malghani, and I. M. Ali. 2010. Microbial biomass, and dissolved organic carbon and nitrogen strongly affect soil respiration in different land uses: A case study at three gorges reservoir area, South China. Agr. Ecosyst. Environ. **137**: 294–307. doi:10.1016/j.agee.2010.02.015

Jarvis, P., and others. 2007. Drying and wetting of Mediterranean soils stimulates decomposition and carbon dioxide emission: The "Birch effect". Tree Physiol. **27**: 929–940. doi:10.1093/treephys/27.7.929

Jones, D. L., and V. B. Willett. 2006. Experimental evaluation of methods to quantify dissolved organic nitrogen (DON) and dissolved organic carbon (DOC) in soil. Soil Biol. Biochem. **38**: 991–999. doi:10.1016/j.soilbio.2005.08.012

Keller, P. S., and others. 2020. Global $CO_2$ emissions from dry inland waters share common drivers across ecosystems. Nat. Commun. **11**: 2126. doi:10.1038/s41467-020-15929-y

Lee, S.-Y., M. E. Ryan, A. F. Hamlet, W. J. Palen, J. J. Lawler, and M. Halabisky. 2015. Projecting the hydrologic impacts of climate change on montane wetlands. PLoS One **10**: e0136385. doi:10.1371/journal.pone.0136385

Lund, J. O., S. A. Wissinger, and B. L. Peckarsky. 2016. Caddisfly behavioral responses to drying cues in temporary ponds: Implications for effects of climate change. Freshw. Sci. **35**: 619–630. doi:10.1086/685583

Marcé, R., B. Obrador, L. Gómez-Gener, N. Catalán, M. Koschorreck, M. I. Arce, G. Singer, and D. von Schiller. 2019. Emissions from dry inland waters are a blind spot in the global carbon cycle. Earth Sci. Rev. **188**: 240–248. doi:10.1016/j.earscirev.2018.11.012

Mavi, M. S. 2018. Evaluation of extractants to quantify dissolved organic carbon and nitrogen in dissimilar soils. J. Indian Soc. Soil Sci. **66**: 111–115. doi:10.5958/0974-0228.2018.00013.0

Nakagawa, S., and H. Schielzeth. 2013. A general and simple method for obtaining $R^2$ from generalized linear mixed-effects models. Methods Ecol. Evol. **4**: 133–142.

Nitzsche, K. N., T. Kalettka, K. Premke, G. Lischeid, A. Gessler, and Z. E. Kayler. 2017. Land-use and hydroperiod affect

kettle hole sediment carbon and nitrogen biogeochemistry. Sci. Total Environ. **574**: 46–56. doi:10.1016/j.scitotenv.2016.09.003

Obrador, B., D. von Schiller, R. Marcé, L. Gómez-Gener, M. Koschorreck, C. Borrego, and N. Catalán. 2018. Dry habitats sustain high CO2 emissions from temporary ponds across seasons. Scientific Reports **8**. doi:10.1038/s41598-018-20969-y

Orchard, V. A., and F. J. Cook. 1983. Relationship between soil respiration and soil moisture. Soil Biol. Biochem. **15**: 447–453. doi:10.1016/0038-0717(83)90010-X

Ostrofsky, M. L., and F. H. Rigler. 1987. Chlorophyll–phosphorus relationships for subarctic lakes in western Canada. Can. J. Fish. Aquat. Sci. **44**: 775–781. doi:10.1139/f87-094

Pinheiro, J., D. Bates, S. DebRoy, and D. Sarkar. 2014. R Core Team (2014) nlme: Linear and nonlinear mixed effects models. R Package Version 3.1-117 [accessed 2018 August 1]. Available from http://CRAN.R-project.org/package=nlme

Post, W. M., W. R. Emanuel, P. J. Zinke, and A. G. Stangenberger. 1982. Soil carbon pools and world life zones. Nature **298**: 156–159. doi:10.1038/298156a0

R Foundation for Statistical Computing. 2017. R: A language and environment for statistical computing.

Raich, J. W., and W. H. Schlesinger. 1992. The global carbon dioxide flux in soil respiration and its relationship to vegetation and climate. Tellus B **44**: 81–99. doi:10.3402/tellusb.v44i2.15428

Reverey, F., L. Ganzert, G. Lischeid, A. Ulrich, K. Premke, and H.-P. Grossart. 2018. Dry-wet cycles of kettle hole sediments leave a microbial and biogeochemical legacy. Sci. Total Environ. **627**: 985–996. doi:10.1016/j.scitotenv.2018.01.220

Rey, A. 2015. Mind the gap: Non-biological processes contributing to soil $CO_2$ efflux. Glob. Chang. Biol. **21**: 1752–1761.

Rice, E. W., R. B. Baird, A. D. Eaton, and L. S. Clesceri. 2018. 5310 Total organic carbon (TOC). *In* Standard methods for the examination of water and wastewater. American Public Health Association.

Robertson, G. P., P. Sollins, B. G. Ellis, and K. Lajtha. 1999. Exchangeable ions, pH, and cation exchange capacity. Standard soil methods for long-term ecological research. Oxford University Press: 106–114.

Rousk, J., P. C. Brookes, and E. Bååth. 2009. Contrasting soil pH effects on fungal and bacterial growth suggest functional redundancy in carbon mineralization. Appl. Environ. Microbiol. **75**: 1589–1596. doi:10.1128/AEM.02775-08

Ryan, M. G., and B. E. Law. 2005. Interpreting, measuring, and modeling soil respiration. Biogeochemistry **73**: 3–27. doi:10.1007/s10533-004-5167-7

Schlesinger, W. H., and J. A. Andrews. 2000. Soil respiration and the global carbon cycle. Biogeochemistry **48**: 7–20.

Serreze, M. C., M. P. Clark, R. L. Armstrong, D. A. McGinnis, and R. S. Pulwarty. 1999. Characteristics of the western United States snowpack from snowpack telemetry ($SNO^{TEL}$) data. Water Resour. Res. **35**: 2145–2160. http://dx.doi.org/10.1029/1999WR900090

Sexstone, G. A., and S. R. Fassnacht. 2014. What drives basin scale spatial variability of snowpack properties in northern Colorado? Cryosphere **8**: 329–344. doi:https://doi.org/10.5194/tc-8-329-2014

Shukla, G., and A. Varma. 2010. Soil enzymology. Springer Science & Business Media.

Skopp, J., M. D. Jawson, and J. W. Doran. 1990. Steady-state aerobic microbial activity as a function of soil water content. Soil Sci. Soc. Am. J. **54**: 1619–1625. doi:10.2136/sssaj1990.03615995005400060018x

Smol, J. P., and M. S. Douglas. 2007. Crossing the final ecological threshold in high Arctic ponds. Proc. Natl. Acad. Sci. **104**: 12395–12397. doi:10.1073/pnas.0702777104

Solórzano, L., and J. H. Sharp. 1980. Determination of total dissolved phosphorus and particulate phosphorus in natural waters1. Limnol. Oceanogr. **25**: 754–758.

Taylor, S., P. J. Gilbert, D. A. Cooke, M. E. Deary, and M. J. Jeffries. 2019. High carbon burial rates by small ponds in the landscape. Front. Ecol. Environ. **17**: 25–31. doi:10.1002/fee.1988

Thomspon, S. 2012. Stratified sampling, p. 139–156. *In* Sampling. John Wiley & Sons.

Trumbore, S. 2000. Age of soil organic matter and soil respiration: Radiocarbon constraints on belowground C dynamics. Ecol. Appl. **10**: 399–411. doi:10.1890/1051-0761(2000)010%5B0399:AOSOMA%5D2.0.CO;27

Weise, L., et al. 2016. Water level changes affect carbon turnover and microbial community composition in lake sediments. FEMS Microbiol. Ecol. **92**. doi:10.1093/femsec/fiw035

Williams, D. D. 1997. Temporary ponds and their invertebrate communities. Aquat. Conserv. Mar. Freshw. Ecosyst. **7**: 105–117. doi:10.1002/(SICI)1099-0755(199706)7:2%3C105::AID-AQC222%3E3.0.CO;2-K

Williamson, C. E., J. E. Saros, W. F. Vincent, and J. P. Smol. 2009. Lakes and reservoirs as sentinels, integrators, and regulators of climate change. Limnol. Oceanogr. **54**: 2273–2282. doi:10.4319/lo.2009.54.6_part_2.2273

Wissinger, S. A., H. H. Whiteman, G. B. Sparks, G. L. Rouse, and W. S. Brown. 1999. Foraging trade-offs along a predator–permanence gradient in subalpine wetlands. Ecology **80**: 2102–2116.

Wissinger, S. A., W. S. Brown, and J. E. Jannot. 2003. Caddisfly life histories along permanence gradients in high-altitude wetlands in Colorado (USA). Freshw. Biol. **48**: 255–270.

Wissinger, S. A., B. Oertli, and V. Rosset. 2016. Invertebrate communities of alpine ponds, p. 55–103. *In* Invertebrates in freshwater wetlands. Springer.

Wissinger, S. A., M. E. Perchik, and A. J. Klemmer. 2018. Role of animal detritivores in the breakdown of emergent plant detritus in temporary ponds. Freshw. Sci. **37**: 826–835. doi: 10.1086/700682

## Acknowledgments

We thank J. Forbes for assistance with field and lab research. We thank the Rocky Mountain Biological Laboratory for logistical support and the Nature Conservancy for access to the Mexican Cut Nature Reserve. Funding for this research was provided by grant #1556914 to B.W.T., grant #1557015 to S.A.W., and partially by grant #1830178 to A.G.D., all from the National Science Foundation. Additional funding for instrumentation and other resources were provided by the Department of Applied Ecology at North Carolina State University to B.W.T.

## Conflict of Interest

None declared.

*Submitted 21 August 2019*
*Revised 02 March 2020*
*Accepted 01 October 2020*

*Associate editor: Edward Stets*

**Supplementary Materials**

$CO_2$ efflux over the season: Methods

In order to estimate the season long efflux from exposed pond sediments, we expanded the analysis performed in DelVecchia et al. (2019) by adding in the montane sites and revising the estimates of sediment $CO_2$ efflux. Because that study included more detailed measurement of pond areas at the subalpine site over the course of the 2017 season, we used the same 2017 areal drying estimates.

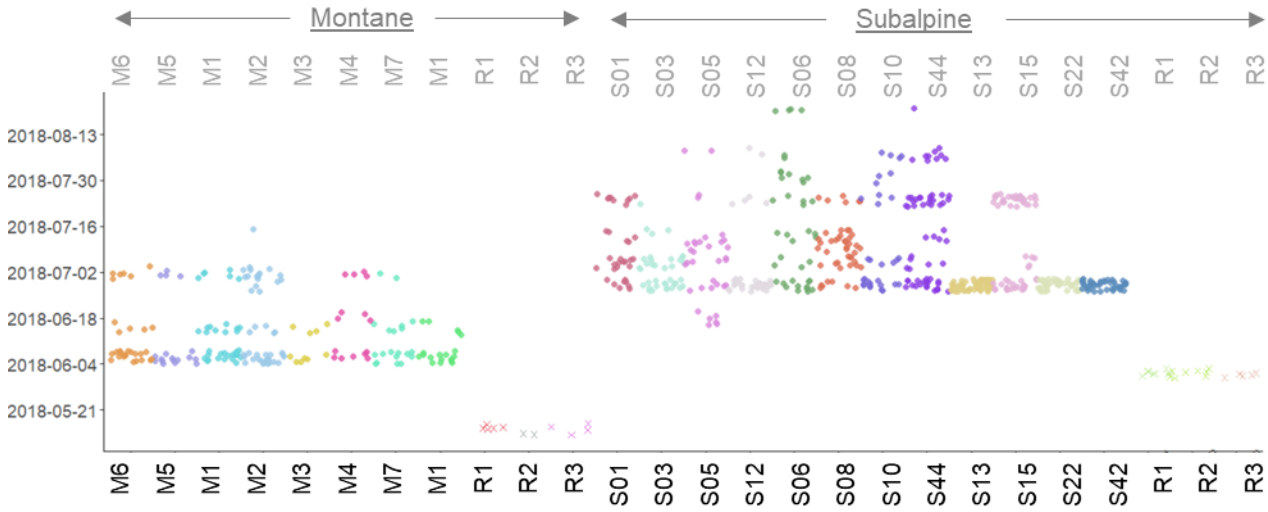
The montane site ponds were either temporary (dried annually) or dried most years, including in 2018. We applied the methods documented in DelVecchia et al. (2019) to assume a linear rate of decrease in pond areas over the time from ice-out to when we observed complete drying. We had observed complete drying in all ponds but M2 and M1, but at the time of the last collar installation, 2 July 2018, the ponds had dried to ~10% of their total areas (by observation, not measured). Instead of using this, we took a more conservative approach by assuming these two ponds did not dry until 28 July 2018, which is the average dry date for pond M2 in years 2012-2013, the only years for which we had sensor-documented drying data for either of these ponds (sensor methods described in DelVecchia et al. 2019).

To estimate season length used in the subalpine ponds, we relied on pond depth sensor data that was available for pond M7, a semi-permanent pond, from 2007 to 2013. The pond dried completely in all of these years. We used the average pond ice out date and re-freeze date (when the pond refilled with snow) to estimate a total season length. No refill events were recorded for M7 over that period, so we assumed that montane ponds did not refill before the freeze date in 2018.

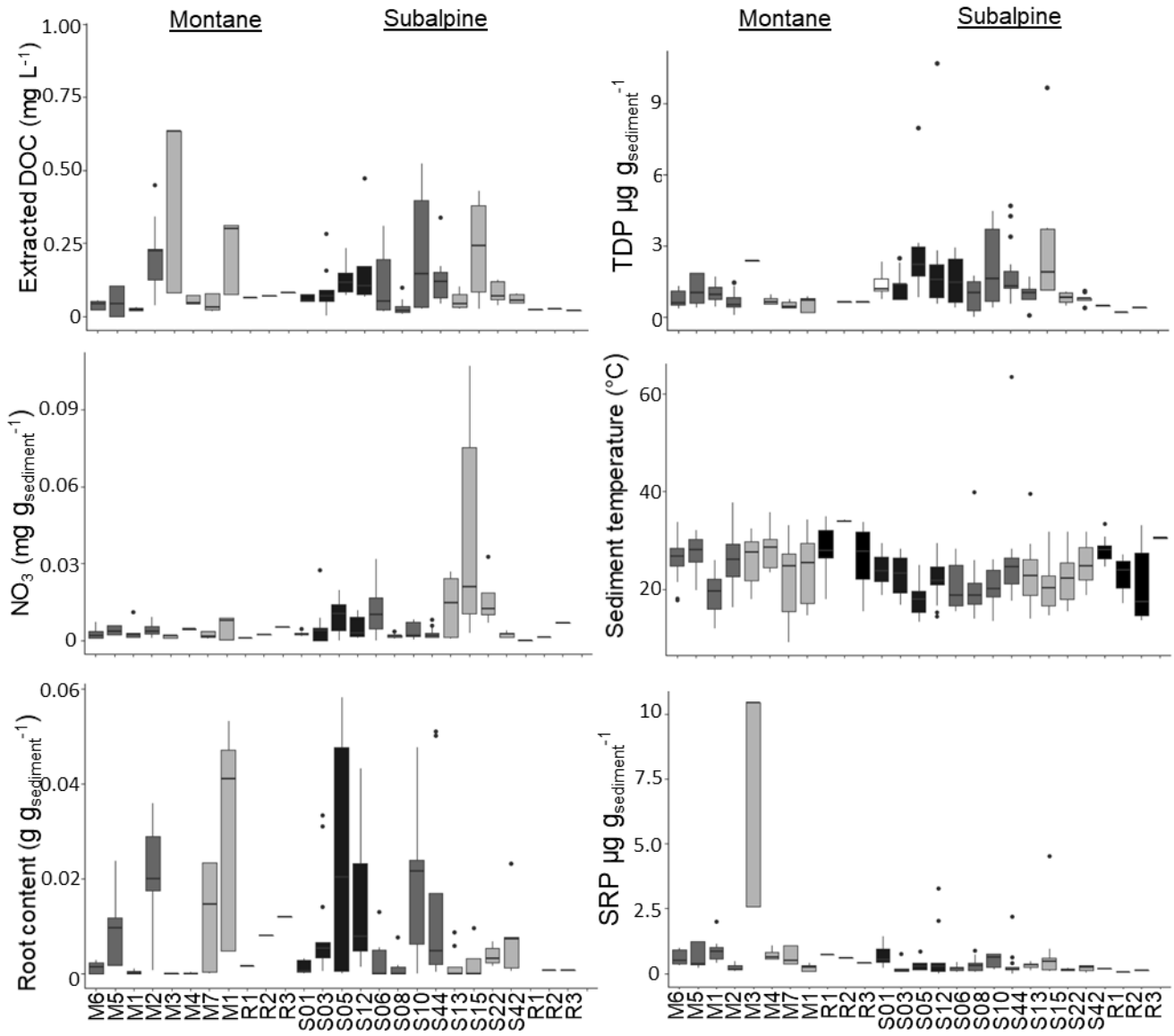
We integrated over the period of drying to estimate total area-days of wetted and dried pond surface area, then multiplied the dried pond area-days by the average sediment $CO_2$ flux rate per pond over that period. Similarly, we used the water $CO_2$ flux rates reported by DelVecchia et al. 2019 to estimate water to atmosphere $CO_2$ flux over that period. To standardize the sediment $CO_2$ flux by pond area, we divided this total season long estimate by total pond area. Averages and standard errors were calculated per pond hydroperiod classification at each site, or per each site.



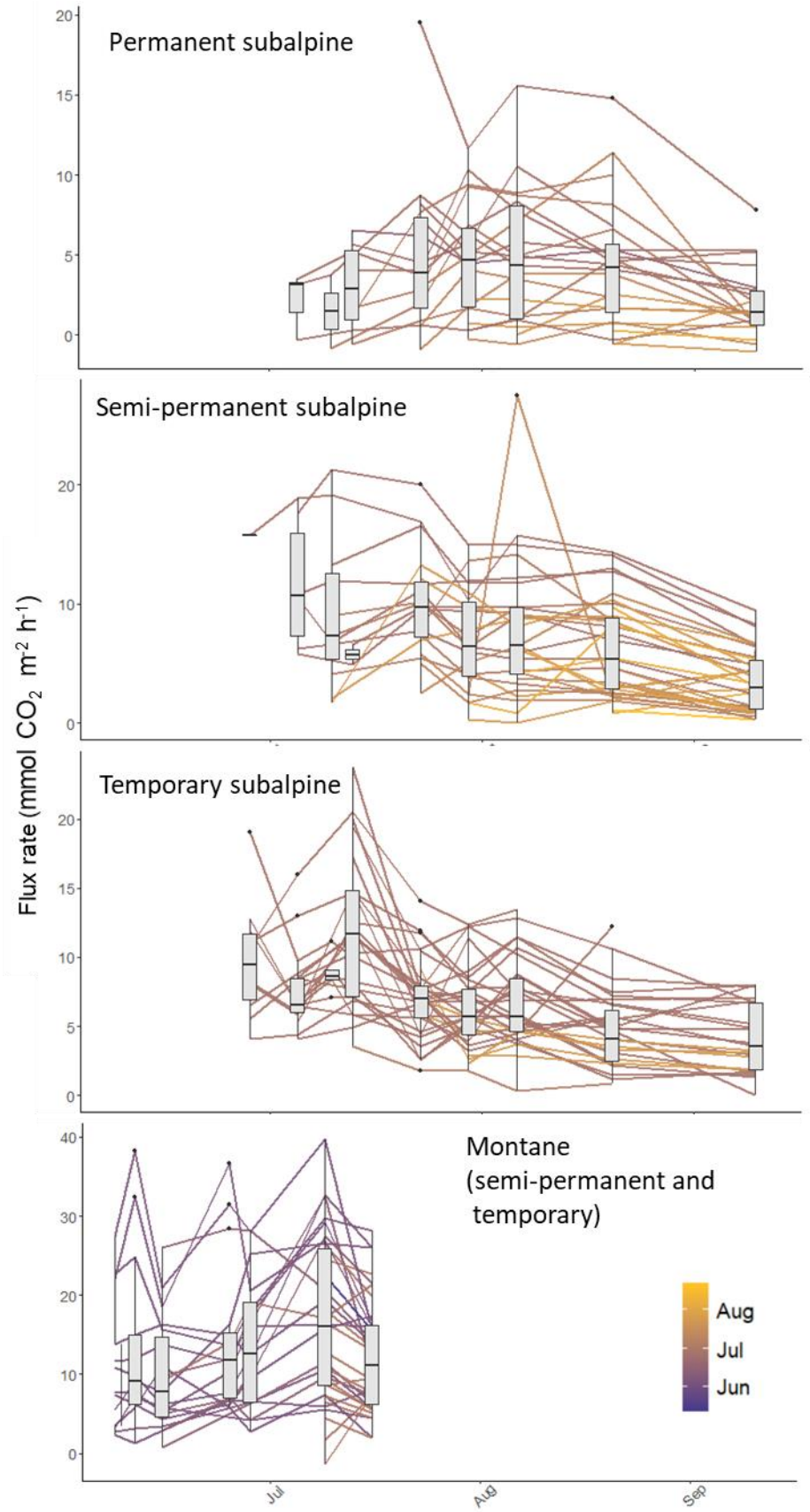
Supplementary Figure 1. In the upper panel a semi-permanent pond (M1) began to dry and expose pond margins to air. As these margins were exposed, we were installed collars in the exposed sediment. In temporary ponds (as in lower picture, S15), the entire pond's surface area was sediment that exposed to air before the end of the season. In all exposed sediment locations, we collected measurements of $CO_2$ flux using the respiration chamber setup shown in the lower panel.



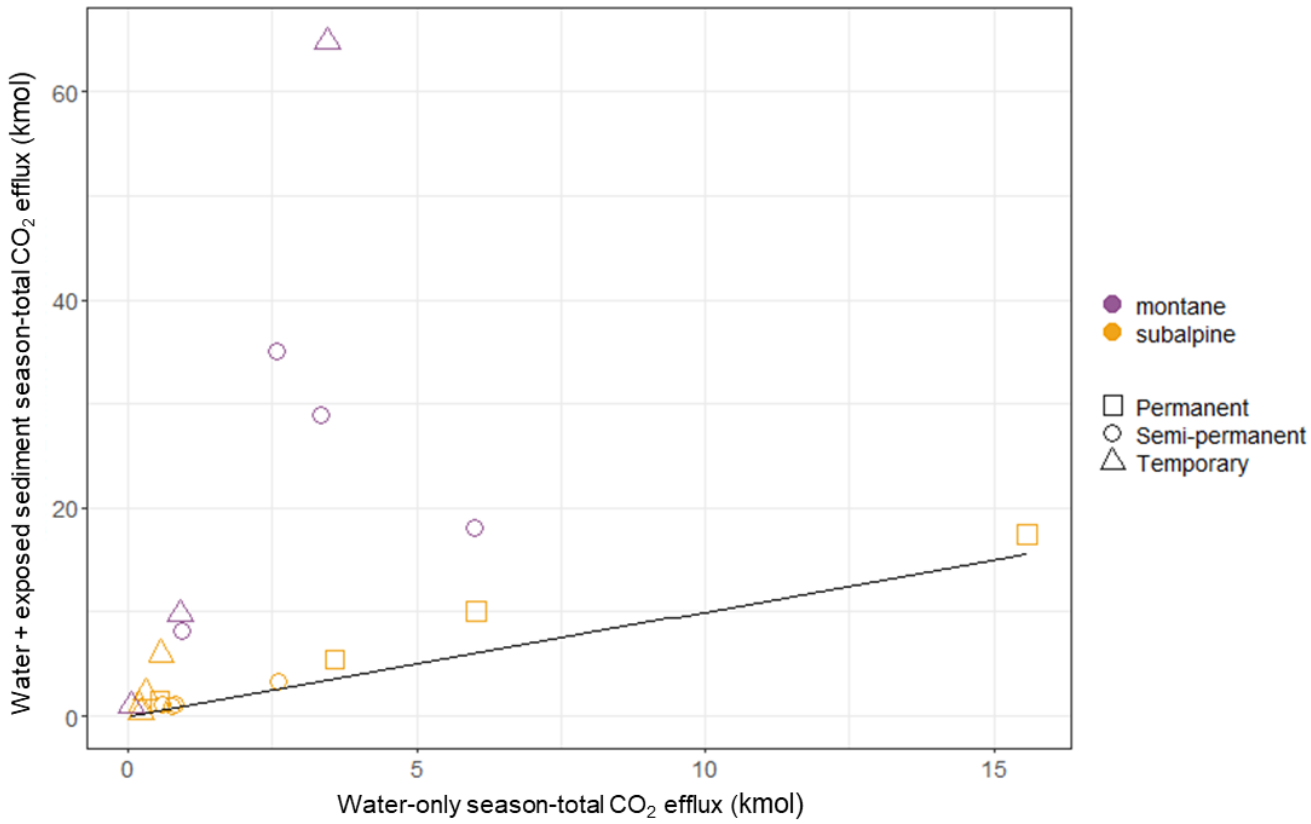

Supplementary Figure 2. Distribution of collars for each pond and dry date. As indicated in Figure 1, collars were placed within margins of the pond as it dried down, so the first collar placement indicates the first time that any pond drying was observed. The last collar placement indicates when the pond dried completely. All montane ponds and all subalpine temporary ponds dried completely over the study period.




Supplementary Figure 3. Boxplots (mean and IQR, dots as outliers) for a subset of variables measured at each collar. Dark boxes are permanent ponds; light boxes are temporary ponds, and lines (no boxes) are raw reference site values. Additional data are shown in Figure 3 and summarized in Table 1 as well as in Supplementary Table 1.


Permanent subalpine
Semi-permanent subalpine
Temporary subalpine
Montane
(semi-permanent and
temporary)
Flux rate (mmol $CO_2$ $m^{-2}$ $h^{-1}$)
Aug
Jul
Jun
Jul
Aug
Sep

Supplementary Figure 4. Individual $CO_2$ flux rates measured at each collar at each sampling date. Boxplots (median and IQR, dots as outliers) are overlaid when multiple collars were sampled on the same day. Lines connecting points from the same collar are colored by the date of collar installation (collars installed later in the season are increasingly yellow)




Supplementary Figure 5. The total kmol $CO_2$ effluxed per pond over a season from both pond water and exposed sediment areas is far higher than what would be expected from water efflux alone. Line indicates 1:1 relationship. M2 is not shown: 380.9 kmol $CO_2$, 70.7 kmol water $CO_2$

SupplementaryTable 1 . Mean +/- SE values for each variable measured at each pond and reference site. $NO_3$ and TDN units are in units of μg $g_{sediment}^{-1}$ for Montane ponds and mg $g_{sediment}^{-1}$ for Subalpine ponds. Reference sites have only one sampling point each.

| Pond | TOC (mg/g) | pH | SRP (µg/g) | TDP (µg/g) | $NO_3$ (*g/g) | TDN (*g/g) | Roots (mg/g) |
|---|---|---|---|---|---|---|---|
| M1 | 0.02 ± 0.00 | 7.07 ± 0.04 | 0.96 ± 0.11 | 1.03 ± 0.08 | 1.60 ± 0.15 | 2.17 ± 0.18 | 0.42 ± 0.00 |
| M5 | 0.05 ± 0.01 | 6.90 ± 0.04 | 0.68 ± 0.06 | 1.19 ± 0.03 | 3.89 ± 0.19 | | 7.96 ± 0.02 |
| M6 | 0.04 ± 0.00 | 6.73 ± 0.05 | 0.61 ± 0.05 | 0.78 ± 0.06 | 2.92 ± 0.53 | 1.45 ± 0.17 | 1.27 ± 0.00 |
| M7 | 0.04 ± 0.00 | 6.62 ± 0.06 | 0.55 ± 0.05 | | 1.87 ± 0.15 | | 12.53 ± 0.02 |
| M2 | 0.21 ± 0.02 | 6.92 ± 0.08 | 0.21 ± 0.02 | 0.62 ± 0.03 | 3.97 ± 0.21 | 9.56 ± 2.47 | 23.92 ± 0.01 |
| M3 | 0.41 ± 0.01 | 6.12 ± 0.08 | 7.29 ± 0.91 | 2.40 ± 0.00 | | 11.64 ± 1.19 | 0.00 ± 0.00 |
| M4 | 0.06 ± 0.00 | 6.71 ± 0.03 | 0.71 ± 0.04 | 0.66 ± 0.03 | 10.94 ± 3.25 | 12.48 ± 1.35 | 0.10 ± 0.00 |
| M8 | 0.22 ± 0.04 | 6.66 ± 0.15 | 0.25 ± 0.04 | 0.60 ± 0.07 | 3.60 ± 1.04 | 8.22 ± 1.74 | 30.19 ± 0.13 |
| MR | 0.0 | | 0.73 | | 0.86 | 4.03 | 1.64 |
| MR | 0.07 | 7.08 | 0.58 | 0.65 | 2.01 | 1.77 | 8.08 |
| MR | 0.08 | 6.46 | 0.41 | 0.64 | 5.02 | 3.37 | 12.00 |
| S01 | 0.06 ± 0.00 | 5.50 ± 0.04 | 0.68 ± 0.1 | 1.42 ± 0.15 | 0.00 ± 0.00 | 0.07 ± 0.00 | 1.43 ± 0.00 |
| S03 | 0.08 ± 0.01 | 5.08 ± 0.04 | 0.14 ± 0.04 | 1.15 ± 0.12 | 0.01 ± 0.00 | 0.07 ± 0.02 | 11.64 ± 0.02 |
| S05 | 0.13 ± 0.01 | 5.35 ± 0.04 | 0.30 ± 0.04 | 2.51 ± 0.35 | 0.01 ± 0.00 | 0.12 ± 0.07 | 25.12 ± 0.07 |
| S12 | 0.17 ± 0.03 | 5.00 ± 0.06 | 0.80 ± 0.28 | 3.01 ± 0.80 | 0.01 ± 0.00 | 0.06 ± 0.04 | 14.58 ± 0.04 |
| S06 | 0.15 ± 0.02 | 4.86 ± 0.05 | 0.24 ± 0.03 | 1.72 ± 0.19 | 0.01 ± 0.00 | 0.06 ± 0.00 | 4.26 ± 0.00 |
| S08 | 0.03 ± 0.00 | 5.37 ± 0.13 | 0.28 ± 0.03 | 0.83 ± 0.06 | 0.00 ± 0.00 | 0.03 ± 0.00 | 1.16 ± 0.00 |
| S10 | 0.24 ± 0.03 | 4.81 ± 0.09 | 0.43 ± 0.04 | 2.34 ± 0.22 | 0.00 ± 0.00 | 0.05 ± 0.05 | 21.14 ± 0.05 |
| S44 | 0.14 ± 0.02 | 5.19 ± 0.05 | 0.33 ± 0.07 | 2.21 ± 0.22 | 0.00 ± 0.00 | 0.07 ± 0.03 | 17.06 ± 0.01 |
| S13 | 0.05 ± 0.00 | 4.90 ± 0.02 | 0.31 ± 0.02 | 1.08 ± 0.09 | 0.01 ± 0.00 | 0.05 ± 0.00 | 2.03 ± 0.00 |
| S15 | 0.28 ± 0.04 | 4.97 ± 0.02 | 0.92 ± 0.23 | 2.98 ± 0.40 | 0.04 ± 0.00 | 0.09 ± 0.00 | 1.92 ± 0.00 |
| S22 | 0.08 ± 0.01 | 5.14 ± 0.05 | 0.14 ± 0.01 | 0.85 ± 0.04 | 0.02 ± 0.00 | 0.05 ± 0.00 | 3.89 ± 0.00 |
| S42 | 0.06 ± 0.00 | 5.76 ± 0.02 | 0.17 ± 0.01 | 0.92 ± 0.02 | 0.00 ± 0.00 | 0.01 ± 0.01 | 6.53 ± 0.01 |
| SR | 0.02 | | 0.19 | 0.49 | 0.00 | 0.03 | |
| SR | 0.02 | 5.19 | 0.05 | 0.22 | 0.00 | 0.02 | 0.70 |
| SR | 0.02 | 5.14 | 0.11 | 0.41 | 0.01 | 0.02 | 0.81 |

Supplementary Table 2. ANOVA was used to validate the use of means stratified by transects, and ponds, and to separate analyses by classifications and sites.

| **Variable** | **Deg. freedom** | **F value** | **Pr(>F)** |
|---|---|---|---|
| Site | 1 | 277.848 | < 2e-16 |
| Classification | 3 | 24.369 | 5.60E-15 |
| Classification:Pond | 17 | 18.265 | < 2e-16 |
| Classification:Pond:Transect | 21 | 4.533 | 1.46E-10 |
| Residuals | 672 | | |

Supplementary Table 3. Loadings are reported for each of the variables included in the principal components analyses presented in Figure 3.

| | Montane PC1 | Montane PC2 | Subalpine PC1 | Subalpine PC2 |
|---|---|---|---|---|
| BD | -0.457 | 0.064 | 0.314 | -0.388 |
| LOI | 0.479 | -0.134 | 0.117 | -0.569 |
| DOC | 0.407 | -0.229 | -0.459 | -0.055 |
| pH | -0.064 | 0.514 | 0.127 | 0.102 |
| SRP | -0.356 | -0.491 | -0.412 | -0.235 |
| TDP | -0.201 | -0.606 | -0.462 | -0.031 |
| $NO_3$ | -0.037 | 0.025 | -0.296 | -0.311 |
| TDN | 0.137 | -0.024 | -0.398 | -0.103 |
| Roots | 0.435 | -0.198 | -0.178 | 0.542 |
| Temperature | 0.125 | 0.113 | 0.013 | 0.233 |

Supplementary Table 4. Season-long efflux estimates (mean ± s.e.) that include both water and sediment efflux as ponds dry down. Season-long efflux is reported standardized by pond areas and by pond with wetted and dry sediment areas included for reference.

| **Site** | **Hydroperiod Classification** | **Area ($m^2$)** | **Season-long total efflux (mol $m^{-2}$)** | **Season-long total efflux (kmol $pond^{-1}$)** |
|---|---|---|---|---|
| Montane | Semi-permanent | 5680 ± 4590 | 23.2 ± 5.2 | 94.2 ± 71.8 |
| Montane | Temporary | 500 ± 350 | 47.0 ± 7.6 | 25.2 ± 20.0 |
| Subalpine | Permanent | 2150 ± 1080 | 5.2 ± 0.9 | 8.6 ± 3.4 |
| Subalpine | Semi-permanent | 460 ± 180 | 3.8 ± 0.4 | 1.6 ± 0.6 |
| Subalpine | Temporary | 130 ± 30 | 15.3 ± 4.6 | 2.4 ± 1.3 |